Click Here for Full Article

Interhourly variability index of geomagnetic activity and its use in deriving the long-term variation of solar wind speed

Leif Svalgaard[1] and Edward W. Cliver[2]

[1] We describe the detailed derivation of the interhourly variability (*IHV*) index of geomagnetic activity. The *IHV* index for a given geomagnetic element is mechanically derived from hourly values or means as the sum of the unsigned differences between adjacent hours over a 7-hour interval centered on local midnight. The index is derived separately for stations in both hemispheres within six longitude sectors spanning the Earth using only local night hours. It is intended as a long-term index and available data allows derivation of the index back well into the 19th century. On a timescale of a 27-day Bartels rotation, *IHV* averages for stations with corrected geomagnetic latitude less than 55° are strongly correlated with midlatitude range indices ($R^2 = 0.96$ for the *am* index since 1959; $R^2 = 0.95$ for the *aa* index since 1980). We find that observed yearly averages of *aa* before the year 1957 are ∼3 nT too small compared to values calculated from *IHV* using the regression constants based on 1980–2004. We interpret this discrepancy as an indication that the calibration of the *aa* index is in error before 1957. There is no systematic discrepancy between observed and similarly calculated *ap* values back to 1932. Bartels rotation averages of *IHV* are also strongly correlated with solar wind parameters ($R^2 = 0.79$ with BV^2). On a timescale of a year combining the *IHV* index (giving BV^2 with $R^2 = 0.93$) and the recently developed interdiurnal variability (*IDV*) index (giving interplanetary magnetic field magnitude, *B*, with $R^2 = 0.74$) allows determination of solar wind speed, *V*, from 1890 to present. Over the ∼120-year series, the yearly mean solar wind speed varied from a low (inferred) of 303 km/s in 1902 to a high (observed) value of 545 km/s in 2003. The calculated yearly values of the product *BV* using *B* and *V* separately derived from *IDV* and *IHV* agree quantitatively with (completely independent) *BV* values derived from the amplitude of the diurnal variation of the horizontal component in the polar caps since 1926 (and sporadically further back).

1. Introduction

[2] Modern geomagnetic indices aim at becoming proxies for solar wind parameters and to be useful in studying the variation with time of the solar wind and, ultimately, the Sun. While direct and systematic measurements of the solar wind extend a little more than 40 years, we have a geomagnetic record more than four times that long. In this paper, we develop a new geomagnetic index, the interhourly variability or *IHV* index, that enables us to bring this extended record to bear on the question of the long-term variation of the solar wind, a topic of increasing interest with impact on a range of solar-heliospheric physics including the solar dynamo, climate change, and cosmic ray modulation [e.g., *Fisk and Schwadron*, 2001; *Cliver et al.*, 1998b; *Caballero-Lopez et al.*, 2004].

1.1. Geomagnetic Indices Bear Witness to Solar Conditions

[3] It was realized long ago [e.g., *Bartels*, 1940] that solar electromagnetic radiation (primarily far ultraviolet, FUV) and solar "corpuscular" radiation (what we today call the "solar wind") give rise to conditions promoting different classes of fluctuations of the geomagnetic field. FUV radiation creates and maintains the lower ionospheric layers. Solar tidal motions of the ionosphere and thermally driven ionospheric winds produce a quasi-regular daily S_R variation by dynamo action. The irregular geomagnetic variations are described or measured by geomagnetic indices that codify and compress the extraordinary complexity of the variations of the geomagnetic field. Modern geomagnetic indices attempt to remove the S_R variation in order to isolate the irregular part ascribed to activity induced by the solar wind [*Mayaud*, 1980]. If this is possible, the index becomes a proxy for solar properties and can be used to study variation with time of the solar wind and the Sun.

[1]ETK, Inc., Houston, Texas, USA.
[2]Space Vehicles Directorate, Air Force Research Laboratory, Hanscom Air Force Base, Bedford, Massachusetts, USA.
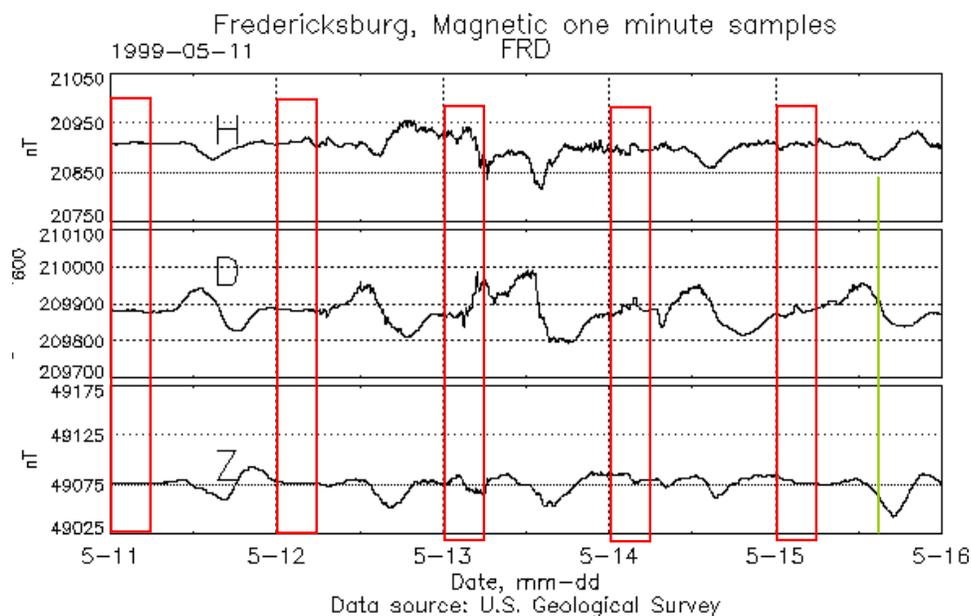
Figure 1. Variation of the geomagnetic elements at Fredericksburg, 11–15 May 1999 (UT). The "effective" noon is marked with a green line on 15 May. The red boxes indicate the 6 hours around midnight where the regular variation is absent or minimal. These intervals are used to define the *IHV* index. A good example of a day with very little activity is 11 May. It is, in fact, the famous day where "the solar wind disappeared" [e.g., *Jordanova et al.*, 2001]. The solar wind momentum flux was only 1% of its usual value and the magnetosphere diameter was five times larger than normal. The interplanetary magnetic field was not affected and had its usual properties. The variability of S_R is clearly seen by comparing 11 May and 15 May.

1.2. *IHV*: A Mechanically Derived Long-Term Geomagnetic Index

[4] Derivation of a geomagnetic range index [*Bartels et al.*, 1939; *Mayaud*, 1967] involves both the ability of the observer to correctly identify the variations not caused by the solar wind and the availability of appropriately inter-calibrated conversion tables. Well-trained observers can obtain a remarkable consistency in scaling K indices. However, observers, stations, and instruments change over time, new conversion tables have to be drawn up and intercalibrated with the previous tables, and the station network thins when we go back in time. The entire process cannot easily or mechanically be duplicated and the quality and stability of calibration of the index values are difficult and labor-intensive to gauge. In the present paper we shall show that the long time series of hourly values of the magnetic components from observatories (some extending back into the 1830s) provide a basis for constructing a new index, the interhourly variability (*IHV*) index, measuring solar wind related activity, without visual inspection of the original magnetograms (many of which may no longer exist or, for eye readings, may never have existed), using a mechanical and readily duplicated derivation process.

1.3. Fundamental Difference Between *IHV* and Other Indices

[5] In deriving the *IHV* index, we follow the suggestion by *Mayaud* [1980] to exclude daytime hours in order to eliminate the influence of the regular variation. Because we are constructing an index for long-term trends, we can largely bypass the problem caused by the solar FUV influence by only using data from the night hours. During the 7 hours around local midnight, the influence of the S_R variation is small and geomagnetic activity is relatively largest. By only using a quarter of each local day, we get an index that for a given station is a statistical sample of the global activity. The sample is biased by any UT variations of activity, but this can be corrected for in a straightforward manner as described below. By combining many stations distributed in longitude in both hemispheres, we aim to construct an index that on a 27-day rotation basis reproduces the *am* index [*Mayaud*, 1967], basically covering the entire geomagnetic record since regular observations began. This procedure is validated a posteriori by the very close correlation between our new index and the high-quality *am* index. While the *am* index is only available since 1959, we obtain *IHV* in the present study back to 1883. Records exist, not yet in digitized electronic format and therefore not yet incorporated into the index, that should make it possible to extend the *IHV* continuously back to the 1830s.

1.4. Use of *IHV* to Derive the Solar Wind Speed

[6] A close relationship between solar wind parameters and the *am* index has been demonstrated by many workers. It is well-established [e.g., *Svalgaard*, 1977; *Feynman and Crooker*, 1978; *Murayama and Hakamada*, 1975; *Lundstedt*, 1984] that geomagnetic range indices (such as
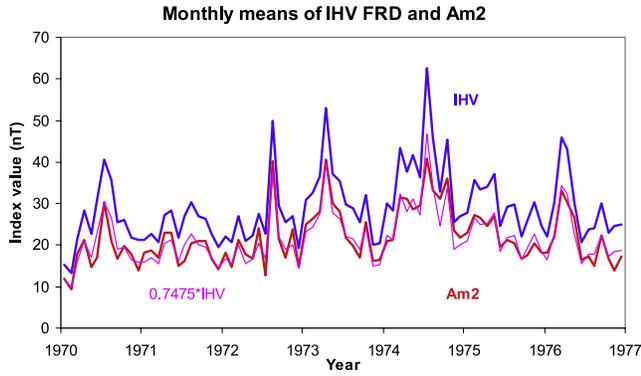
Figure 2. Comparison of monthly means of the "raw" *IHV* index (blue) calculated for the H component at Fredericksburg and the *Am2* index (red) for the interval 1970–1976. The year labels on the abscissa mark the beginning of each year. The thin pink curve shows *IHV* scaled down by 0.7475 for direct comparison with *Am2*. Note that *Am2* is the average *am* index for two 3-hour intervals.

am) are robustly correlated with the product BV^2, where B is the magnitude of the interplanetary magnetic field impinging on the Earth with solar wind speed V. We can therefore determine the product BV^2 from geomagnetic indices, including *IHV*. To make further progress, we must separate the influence of the two parameters B and V. That, then, is the basic problem to be solved, as was realized by *Feynman and Crooker* [1978]. *Lockwood et al.* [1999] attempted to determine V from an ad hoc formula involving the *aa* index and the Sargent recurrence index [*Sargent*, 1986]. Although this approach worked well for the initial dataset employed, it failed when new data became available [*Svalgaard and Cliver*, 2006]. In the present study, we will use B derived directly from our interdiurnal variability index (*IDV*) [*Svalgaard and Cliver*, 2005] to obtain V from BV^2 (*IHV*). We also use the product BV derived from polar cap diurnal variations [*Le Sager and Svalgaard*, 2004] as a divisor for BV^2 to obtain an independent V series with which to check that obtained by our primary method.

1.5. Why Not Use the Long-Term *aa* Index?

[7] *Mayaud* [1972, 1973, 1980] established the *aa* index as the standard measure of long-term geomagnetic variability. This index, based on observations from two nearly antipodal midlatitude stations, one each in Australia and England, extends from 1868 to present. The *aa* index, which has an extension to 1844 [*Nevanlinna*, 2004], has been used in a variety of studies of long-term solar and solar-terrestrial variability, in particular, first by *Svalgaard* [1977] and then perhaps most notably by *Lockwood et al.* [1999] to infer a more than doubling of the solar coronal magnetic field during the 20th century, claims that we cannot substantiate. These studies and numerous others [e.g., *Feynman and Crooker*, 1978; *Cliver et al.*, 1998a] assume a correct calibration of *aa* over time. Because of the growing use of the *aa* index for our understanding of long-term solar behavior, it is important to verify the long-term stability of its calibration. The *IHV* index is based on many more stations than the *aa* index and permits comparisons

between several stations over extended periods of time rather than just between the single pair of stations over only 2 years that Mayaud used to calibrate *aa* after station changes. We confirm in the present paper several recent independent findings (*Jarvis* [2005], *Mursula and Martini* [2006], and M. Lockwood et al., The long-term drift in geomagnetic activity: calibration of the aa index using data from a variety of magnetometer stations, submitted to *Annales Geophysicae*, 2007, hereinafter referred to as Lockwood et al., submitted manuscript, 2007) following the preliminary work by *Svalgaard et al.* [2003, 2004]) that the *aa* index does not have stable calibration, is in need of revision, and is therefore, in its present version, not suitable for deriving quantitative information about long-term changes in the solar wind or the Sun.

1.6. Roadmap

[8] After providing a detailed derivation of the *IHV* index in sections 2–4 (with corresponding technical aspects discussed in Appendices A and B), we compare the *IHV* with the midlatitude range indices, *am*, *ap*, and *aa*, in section 5. In section 6 we use the *IHV* index to derive solar wind speed from 1890 to present. We then substantiate this result by comparison with inferred solar wind parameters based on the polar cap potential back to 1926 and sporadically to earlier times.

2. Definition of the *IHV* Index
2.1. Historical Background

[9] The *IHV* index springs from the same source as the classical *u*-measure [*Bartels*, 1932], building on concepts by *Broun* [1861] and *Moos* [1910] who defined the interdiurnal variability U of the horizontal component at a given station as the difference between the mean values for that day and for the preceding day taken without regard to sign. The δ index defined by *Chernosky* [1960] was a generalization of this interinterval variability index, where δ could be taken as any value, not just 1 day or 1 hour. Both the u measure and the δ index suffer from contamination from S_R. *Chernosky* [1983] attempted to eliminate S_R by computing the unsigned difference between corresponding 3-hourly means on successive days but was only partly successful because S_R itself varies from day to day. Our solution is more radical as our aim is somewhat lower. We do not attempt to construct an index value for every hour or 3 hours or even a day but are content with a statistical sample based on the 1/4 of the data when S_R is not present. Such a sample can be expected to provide a reliable estimate of the average level of activity for intervals of weeks or longer and will be almost free from contamination by S_R.

2.2. Interhour Variability

[10] The *IHV* index is defined as the sum of the differences, without regard to the sign, of hourly means (or values) for a geomagnetic component from one hour to the next over the 7-hour interval around local midnight where the S_R variation is absent:

$$IHV^{H}(\text{nT}) = \sum_{h=h1}^{h=h1+5} \text{abs } (H_h - H_{h+1}) \qquad (1)$$

Table 1. Geomagnetic Observatories Used in the Present Study[a]

IAGA	Name	GG Long	GG Lat	Midnight	Skip	CGM Lat	From	To	From	To
VLJ	Val Joyeux	2.0	48.8	23.9	21	44.9	1900	1936	1923	1936
CLF	Chambon-la-Foret	2.3	48.1	23.8	21	44.0	1935	2005	1936	2005
DBN	De Bilt, Nederland	5.2	52.1	23.7	20	48.5	1903	1938	1903	1938
WIT	Wittingen	6.8	52.8	23.5	20	49.2	1938	1984	1938	1984
WLH	Wilhelmshafen	8.2	53.5	23.5	20	50.8	1883	1911	1883	1895
WNG	Wingst	9.1	53.7	23.4	20	50.1	1939	2006	1943	2003
FUR	Furstenfeldbruck	11.3	48.2	23.2	20	43.5	1939	2006	1940	2004
BFE	Brorfelde	11.7	55.4	23.2	20	51.8	1981	2006	1981	2004
RSV	Rude Skov	12.5	55.5	23.2	20	51.9	1907	1981	1927	1981
NGK	Niemegk	12.7	52.1	23.2	20	48.0	1932	2006	1932	2004
SED	Seddin	13.0	52.3	23.1	20	48.2	1908	1931	1908	1931
POT	Potsdam	13.1	52.4	23.1	20	48.3	1890	1907	1890	1907
TSU	Tsumeb	17.6	−19.2	22.8	20	−29.4	1964	2006	1964	2004
CTO	Cape Town	18.5	−34.0	22.8	20	−41.5	1932	1940	1932	1940
BNG	Bangui	18.6	4.4	22.8	20	−8.3	1952	2006	1955	2003
HER	Hermanus	19.2	−34.4	22.7	20	−41.8	1941	2006	1941	2004
HBK	Hartebeesthoek	27.7	−25.9	22.2	19	−27.1	1973	2006	1973	2004
AAE	Addis Ababa	38.8	9.0	21.4	18	−0.2	1958	2006	1958	2004
TFS	Tbilisi	44.7	42.1	21.0	18	36.8	1938	2006	1957	2001
CZT	Crozet	51.9	−46.4	20.5	18	−53.2	1974	2004	1974	2004
ARS	Arti	58.6	56.4	20.1	17	51.7	1973	2006	1973	2002
SVD	Sverdlovsk	61.1	56.7	19.9	17	51.9	1929	1980	1930	1980
TKT	Tashkent	69.6	41.3	19.4	17	36.0	1883	1991	1957	1991
PAF	Port aux Francais	70.3	−49.4	19.3	17	−58.5	1957	2006	1957	2004
ABG	Alibag	72.9	18.6	19.1	16	11.3	1904	2006	1925	2004
AAA	Alma-Ata	76.9	43.3	18.9	16	37.9	1963	2002	1963	2002
TRD	Trivandrum	77.0	8.5	18.9	16	0.0	1854	2006	1957	1999
AMS	Martin de Vivies	77.6	−37.8	18.8	16	−46.5	1981	2006	1981	2004
NVS	Novosibirsk	82.9	55.0	18.5	15	49.9	1967	2006	1967	2005
ANN	Annamalainagar	79.7	11.4	18.7	16	3.0	1957	1999	1964	1999
LRM	Learmonth	114.1	−22.2	16.4	13	−33.4	1988	2006	1990	2004
WAT	Watheroo	115.9	−30.3	16.3	13	−42.7	1919	1959	1919	1958
GNA	Gnangara	116.0	−31.8	16.3	13	−44.4	1957	2006	1957	2002
SSH	She-Shan	121.2	31.1	15.9	13	24.0	1932	2006	1932	2002
KNY	Kanoya	130.9	31.4	15.3	13	24.1	1958	2006	1958	2006
ASP	Alice Springs	133.9	−23.8	15.1	13	−34.2	1992	2006	1992	2004
TOK	Tokyo	139.7	35.8	14.7	12	26.7	1897	1912	1897	1912
KAK	Kakioka	140.2	36.2	14.7	12	28.7	1913	2006	1913	2006
MMB	Memambetsu	144.2	43.9	14.4	12	36.5	1950	2006	1957	2006
GUA	Guam	144.9	13.6	14.3	11	5.4	1957	2006	1957	2004
TOO	Toolangi	145.5	−37.5	14.3	11	−48.6	1919	1979	1924	1979
CNB	Canberra	149.4	−35.3	14.0	11	−45.7	1979	2006	1979	2004
EYR	Eyrewell	172.4	−43.4	12.5	10	−50.2	1978	2006	1978	2004
AML	Amberley	172.7	−43.2	12.5	10	−49.9	1929	1977	1957	1977
MID	Midway	182.6	28.2	11.8	9	24.7	2000	2002	2000	2002
API	Apia	188.2	−13.8	11.5	8	−16.0	1905	2006	1922	2004
HON	Honolulu	201.9	21.3	10.5	8	21.7	1902	2006	1902	2004
PPT	Pamatai	210.4	−17.6	10.0	7	−16.3	1968	2006	1968	2004
VIC	Victoria	236.6	48.5	8.2	5	54.2	1956	2006	1957	2004
FRN	Fresno	240.3	37.1	8.0	5	43.6	1982	2006	1983	2004
TUC	Tucson	249.2	32.2	7.4	4	39.9	1909	2006	1909	2002
BOU	Boulder	254.8	40.1	7.0	4	48.5	1964	2006	1967	2004
FRD	Fredericksburg	282.6	38.2	5.2	1	50.3	1956	2006	1956	2004
CLH	Cheltenham	283.2	38.7	5.1	1	50.8	1901	1956	1901	1956
HUA	Huancao	284.7	−12.0	5.0	2	1.2	1922	2006	1922	2004
SJG	San Juan, PR	293.8	18.1	4.4	1	30.0	1926	2006	1926	2004
LQA	La Quiaca	294.4	−22.1	4.4	1	−9.8	1920	1983	1968	1981
VQS	Vieques	294.5	18.3	4.4	1	30.1	1903	1924	1903	1924
TRW	Trelew	294.7	−43.3	4.4	1	−32.9	1957	2006	1957	2004
AIA	Argentine Islands	295.7	−65.3	4.3	1	−50.3	1957	2006	1957	2004
PIL	Pilar	296.1	−31.7	4.3	1	−17.6	1905	2006	1941	1985
LIV	Livingstone Isl.	299.6	−62.7	4.0	1	−48.0	1997	2006	1997	2005
ARC	Arctowski	301.5	−62.2	3.9	1	−47.6	1978	1995	1978	1995
PST	Port Stanley	302.1	−51.7	3.9	0	−38.1	1994	2006	1994	2004
VSS	Vassouras	316.3	−22.4	2.9	23	−14.7	1915	2006	1915	2004
SGE	South Georgia	324.0	−54.5	2.4	22	−44.4	1975	1982	1975	1982
HAD	Hartland	355.5	51.0	0.3	21	48.2	1957	2006	1957	2004
ABN	Abinger	359.6	51.2	0.0	21	48.0	1925	1958	1926	1956
ESK	Eskdalemuir	356.2	55.3	0.3	21	53.1	1908	2006	1911	2004

Table 1. (continued)

IAGA	Name	GG Long	GG Lat	Midnight	Skip	CGM Lat	From	To	From	To
LER	Lerwick	358.8	60.1	0.1	21	58.1	1923	2006	1926	2004
SOD	Sodankylä	26.6	67.4	22.2	19	63.6	1914	2006	1914	2004

[a]Listed are geographic longitude and latitude, UT time of local geographic midnight, the number of hours to skip to reach the 6-hour interval used to calculate *IHV* (see section 3.1), corrected geomagnetic latitude (for the middle of the operating interval), the operating years interval, and the interval for which digital data were available at the time of writing.

where $h1$ is the starting UT hour (0 to 23) of the interval. The hour h should be counted modulo 24 to wrap around to the following day, if needed. H_h is the hourly mean value for the hth hour. If any of the hours in the interval does not have data, the *IHV* value is not calculated for that day. The *IHV* index can be defined for any geomagnetic component (H, D, Z, X, Y, I, F) which may be denoted in an appropriate way, e.g., IHV^H for *IHV* derived from the H component, which is what we concentrate on in the present paper. We refer to *Jonkers et al.* [2003] for definition of geomagnetic components, their relationships, and historical details of their measurement. Components that are expressed as angles must be converted to force units (e.g., D (nT) = H (nT) · D (tenth of arc minutes)/34377). The *IHV* index must be calculated from data values given or properly rounded [*Ellis*, 1900] to the nearest 1 nT. The *IHV* index for a given station is computed as one value for the UT day that contains roughly local midnight (see section 3.1) but is not a daily index, as we only sample part of the day. An average over an interval of many day values (e.g., over a month or a 27-day Bartels rotation) is expected to approximate the average activity over the interval because geomagnetic activity has a high degree of conservation [*Chapman and Bartels*, 1940, p. 585].

2.3. Demonstration of *IHV* Determination for a Single Station

[11] The geomagnetic observatory at Fredericksburg, Virginia (FRD) has been in operation since 1956 (with a brief data availability gap 1981–1983). This observatory is located close to the ideal geomagnetic latitude of 50° for discerning the class of activity used in derivation of the *am*
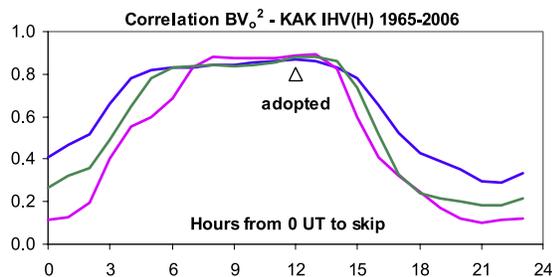
index (and is, in fact, one of the stations contributing to the *am* index, and to the *ap* index, as well).

[12] Figure 1 shows the variation of the three components (H, D, and Z) for several days in May 1999. The S_R variation is clearly seen, including its day-to-day variability. An "effective" noon can be defined as the time where the H component has its maximum excursion. This is also the time when the excursion in the D component changes sign. An
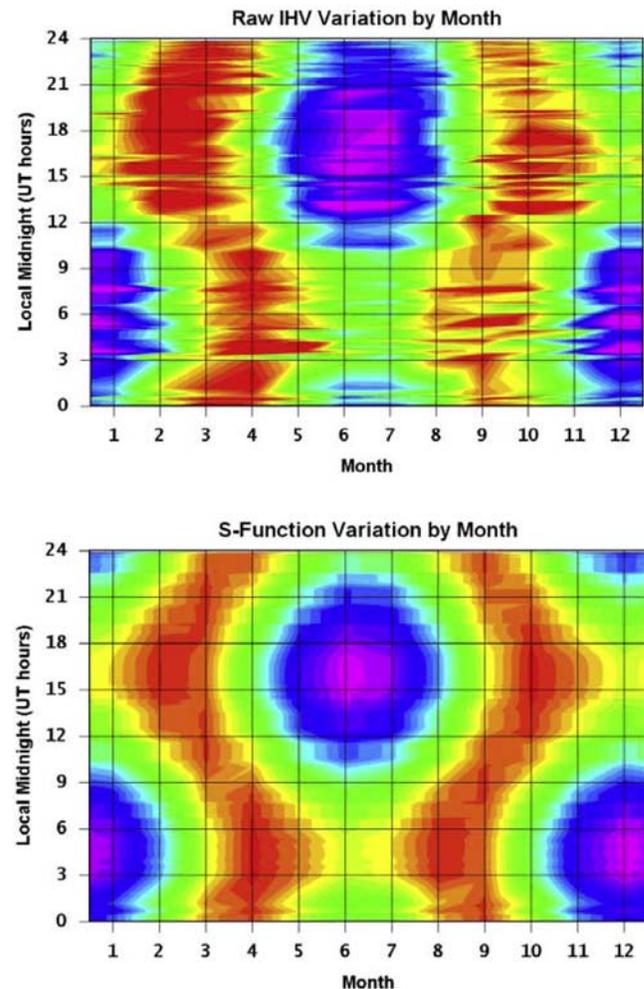

Figure 3. Correlation between yearly averages of *IHV* calculated for KAK for the interval 1965–2006 and the quantity BV^2 (see section 6.2) as a function of the number of hours from 0000 UT to skip before calculating *IHV*. Blue curve is for the H-component, green for the Z-component, and pink for the D-component. The triangle shows the correlation for the number of "skip hours" adopted for this station (12 in this case).

Figure 4. Variation of the *S* function (bottom) and of "raw" *IHV* (top) with month of year and universal time calculated for all the stations in Table 1 for all data available for each station. The *IHV* values for a given station were assigned to the universal time of local midnight. All values were divided by the average values for each station. The color coding over the ~40% variation is chosen such that purple to red represents low to high values.
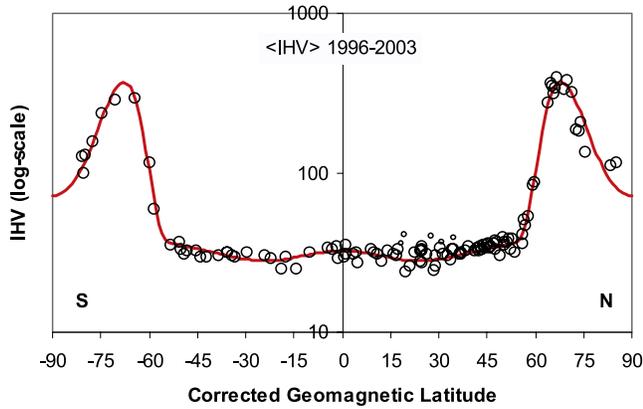
Figure 5. Variation of *IHV* with corrected geomagnetic latitude. Average *IHV* over the interval 1996–2003 for each station with data in that interval are plotted. A few "outliers" (SIL, KRC, QSB, GLM, and KSH) are shown with small circles. Local induction effects may be responsible for these stations having about 25% higher *IHV*. The red curve shows a model fit to the larger circles as described in the text.

effective midnight is then 12 hours away. It is evident for this station, that 0000–0600 UT is a suitable interval for calculation of the *IHV* value as the S_R variation is minimal during this time. We have preliminarily chosen this interval (although in the end we use an interval starting 1 hour later for FRD; see section 3.1) because it just contains the first two 3-hour intervals of the UT day. We can thus readily compare our *IHV* values with the corresponding *am* values. We can compute the average *am* value over the 6-hour interval for the day for direct comparison with the *IHV* value for the day. We denote this average value by *Am2* to distinguish it from the daily average (not to be confused with the average over 2 days).

[13] Figure 2 shows how well our new index compares to the *Am2* index on a timescale of a month over the (arbitrary) interval 1970–1976. The *IHV* index has a high correlation with the *Am2* index (coefficient of determination $R^2 = 0.88$). This close agreement between the two indices even on a timescale as short as a month is the primary argument for the validity of our approach. For a timescale of 1 day, R^2 is still as high as 0.74. The finding that a single station for a limited local time range suffices to fairly characterize global geomagnetic activity during that time is well known and is also the underlying rationale behind the *aa* index.

3. Selection of Stations, Local Time Interval, Data, and Sectors

[14] Table 1 shows coordinates and dates of availability for the stations selected for this study. We have shown that a useful index can be derived from even a single station regardless of its location, as long as it is well equatorward of the auroral zones (section 3.3). The stations shown in Table 1 have been selected based on the availability of electronically readable hourly data from the World Data Centers for Geomagnetism, the INTERMAGNET program, and other sources. More data exist (in yearbooks and observatory reports) but are typically not yet available in

electronic form. In this section we detail the criteria for choosing the local time interval, latitude regions appropriate for *IHV*, and longitudinal sectors, as well as the method used to compensate for the UT variation of geomagnetic activity (undesirable in an index aimed at being a proxy for solar conditions).

3.1. Selection of Interval During the Night

[15] Because the regular diurnal variation is controlled mainly by the Sun's zenith angle, we use the 6-hour interval centered on ordinary geographical midnight, rather than using geomagnetic midnight. The difference is only important at high latitudes where, as we shall see, *IHV*, like the *K* index, should not be used anyway in the meaning of a subauroral zone index. The data available to us are described in the WDC format as "hourly means centered on the universal time half-hours." In reality, the 24 values per day may refer to hourly means centered on the half-hour, or on the whole-hour, or to instantaneous values measured on the whole-hour, or the half-hour. Moreover, "hour" may refer to UT, local standard time, true local time, "Astronomical" time, or even Göttingen time. These variations (at times unknown and inferable only from the data themselves by determining the time of "effective" noon from the diurnal variation by visual inspection) make it difficult to devise a hard rule for assigning the time of the interval to use. The solution we have chosen is to manually assign a number of "hourly" data values to skip at the start of a time series for a given station (purportedly starting as an hourly mean centered on 0030 UT and labeled as hour 00) to align the series with "the 6-hour interval around local geographic midnight" determined by visual inspection of the data. This number is usually within 1 hour of the time, *h*, calculated from *h* = (rounded (24 − longitude/15) − 3) modulo 24, and is given in Table 1 as well. The values of *IHV* are not very sensitive to small variations of the exact starting time of the interval as can be seen from Figure 3. Using a result from section 6.2, namely that *IHV* is strongly correlated with the quantity BV^2 calculated from observed values of the IMF magnitude, *B*, and the solar wind speed, *V*, we show the coefficient of determination, R^2, as a function of the number of hours to skip for the Kakioka observatory (KAK) to obtain optimum correlation. Note the very broad maximum showing the insensitivity of the precise number of hours to skip, as long as the value chosen is within the broad range of high correlation.

[16] After skipping to the beginning of the 6-hour interval, the following 7 hours are then used to calculate six unsigned successive differences between the hourly data; we referred to this as the "6-hour" interval. Their sum is the "raw" *IHV* value for the UT day containing the forth hourly

Table 2. Model Coefficients for Equation (3): Amplitude a_k, Exponent b_k, and Latitude φ_k in Degrees

k	a_k	b_k	$\varphi_k°$
1	0.218	10	0
2	0.728	0.04	23.5
3	9.700	435	68
4	0.408	6	90

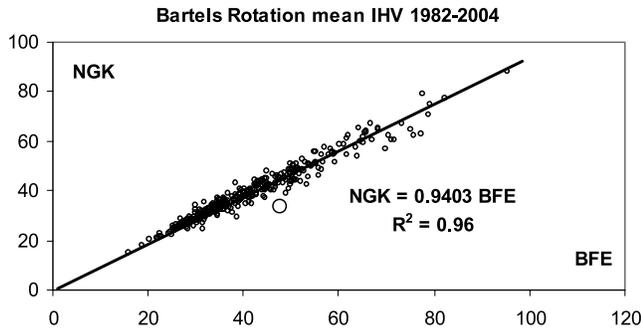**Bartels Rotation mean IHV 1982-2004**

Figure 6. Bartels rotation means of *IHV* for BFE versus NGK for 1982–2004. The scale factor is derived as the slope of the regression line constrained to go through the origin. A single outlier marked with a large circle is not included in the fit.

data point. If any of the seven data values are designated as "missing," *IHV* is considered missing for that day. Finally, we skip over the $24 - 7 = 17$ following hourly data points, positioning to the next 6-hour interval and repeat the procedure until the end of the data set. We assume that intermittent missing data are marked by a special value rather than by the absence of data entries.

3.2. Removing Universal Time Variation

[17] *Svalgaard* [1977], *Svalgaard et al.* [2002] and references therein, and *O'Brien and McPherron* [2002] show that the equinoctial mechanism component of the semiannual variation of geomagnetic activity (e.g., as expressed by the *am* index) can be closely described as a modulation of existing activity by a function of the form

$$(1 + 3 \cos^2 \Psi)^{-2/3} = S(\Psi) \qquad (2)$$

where Ψ is the angle between the solar wind flow direction and the Earth's magnetic dipole axis. The function $S(\Psi)$ varies both with the day of the year and with universal time (UT), and also very slowly due to secular variation of the geomagnetic field and (slower yet) the Earth's orbital elements; the total secular variation of S since 1800 does not exceed 1% and thus is not yet measurable. Figure 4 shows the variation of the S function (bottom) and of the "raw" *IHV* (top) with month of year and universal time calculated for all the stations in Table 1, for all data available for each station. The *IHV* values for a given station were assigned to the universal time of local midnight for that station. All values were divided by the average values for each station to make them comparable. The diminution of activity at the solstices when the geomagnetic pole on the sunward side comes closest to the subsolar point is clearly seen. Indeed, the variations of S and of *IHV* are quantitatively very similar, suggesting that we may remove the equinoctial mechanism part of the UT variation of *IHV* by the simple expedient of dividing by S for the average UT time for each single value of the differences defining *IHV* for each station and for each day. Removing this UT variation minimizes the ill effect of (the inevitable) uneven station distribution. In

the polar caps the UT variation is small and is swamped by the large seasonal variation caused by the variation of ionospheric conductivity, being much higher during local summer. As we shall see, the *IHV* index should not be used for stations within the polar cap, so removal of the UT variation for such stations is moot.

[18] Several workers [e.g., *Svalgaard et al.*, 2002; *Cliver et al.*, 2000; *Crooker and Siscoe*, 1986] have suggested that typically some 25% of the semiannual variation is caused by other mechanisms than the equinoctial effect, possibly related to external causes (variations of solar wind properties with heliographic latitude (axial mechanisms) or to the angle between the magnetic axes of the Sun and the Earth (Russell-McPherron effect)). On rare occasions (e.g., during 1954), these effects can be large or even dominant [*Cliver et al.*, 2004]. We leave those external variations in the index.

3.3. Latitudinal Variation of the *IHV* Index

[19] To get maximal spatial coverage, we computed IHV^H freed from the Ψ-related variation as described in section 3.2 for all 128 stations which had submitted data to the WDCs for the interval 1996–2003, covering most of a solar cycle. Since there were missing data at some stations at different times, the following procedure was used to make the data comparable. The stations were divided into six longitudinal sectors centered on (east) longitudes 15°, 75°, 130°, 200°, 240°, and 290°. $\langle IHV \rangle$ was computed for the H component for each station as a mean over 27-day Bartels rotations for which 20 or more days had data. Within each longitude sector a reference station was chosen that had good data coverage. The Bartels rotation averages for all stations within a sector were then normalized to the reference station (by dividing by $\langle IHV \rangle$ for the reference station). The overall averages $\langle IHV \rangle$ covering the full 8-year interval for the reference stations were then themselves normalized to the overall $\langle IHV \rangle$ for NGK, and each station finally normalized to that same standard by multiplying by the normalized reference averages. The meaningful application of such a procedure relies on the assumption that *IHV* values at different stations are related through a simple constant of proportionality. This assumption is found to hold to a degree of accuracy, arguably good enough for the purpose of establishing the variation of *IHV* with latitude.

Table 3. Scaling Factors for Each Longitude Sector Relative to Sector 15°N[a]

From	IHV15N	R^2	Time
IHV15N	1.0000	1.00	1890–2006
IHV15S	1.0022	0.84	1932–2004
IHV75N	1.2335	0.77	1925–2004
IHV75S	1.2926	0.77	1957–2004
IHV130N	1.4563	0.63	1913–2006
IHV130S	1.3446	0.60	1919–2004
IHV200N	1.5445	0.59	1902–2004
IHV200S	1.5146	0.43	1922–2004
IHV240N	1.1188	0.60	1910–2004
IHV240S	1.3333	N/A	1964–1964
IHV290N	1.1969	0.73	1903–2004
IHV290S	1.2202	0.60	1915–2005

[a]R2 is the coefficient of determination for the correlation between each sector and IHV15N for the time interval given.
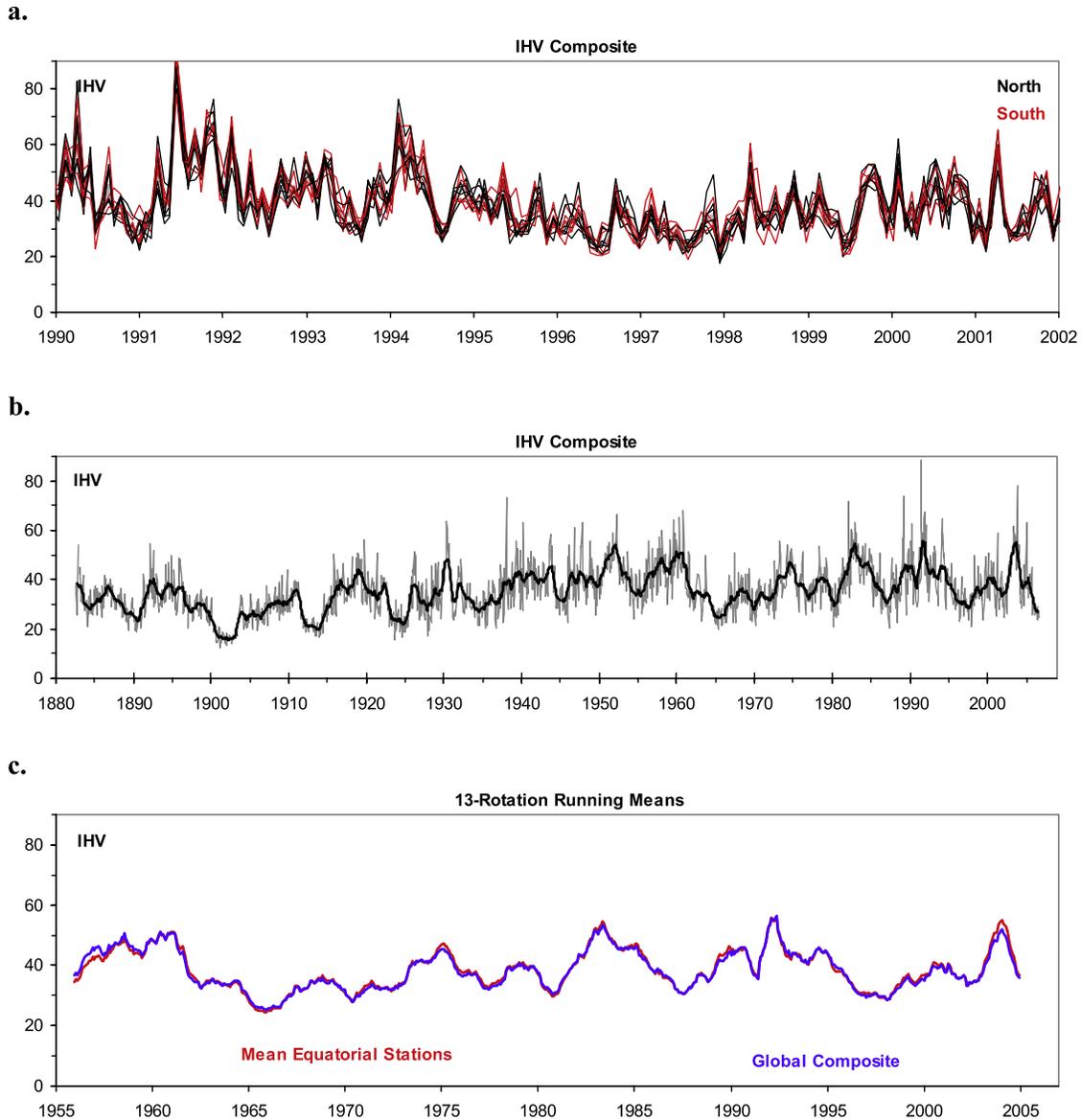
a.

b.

c.

Figure 7. (top) Plot of a portion (years 1990–2001) of all the individual data series that went into the composite series. Northern sectors are shown in black while southern sectors are shown in red. (middle) Plot of the full series for years 1883–2006 (grey curve) overlain by its 13-rotation running mean (heavy black curve). The curve before 1890 is based on preliminary data from BTV and WLH. (bottom) Plot of 13-rotation running means of the composite *IHV* (blue) and *IHV* derived from equatorial stations (red).

[20] Plotting the normalized $\langle IHV \rangle$ for all stations against their corrected geomagnetic latitude, we obtain Figure 5. Other measures of latitude (geographic, simple geomagnetic, dip) result in larger scatter. It is evident that the latitudinal variation is weak below corrected geomagnetic latitude 55° but that *IHV* increases sharply (by an order of magnitude) on the poleward side of that latitude. Distance from the auroral zone seems to be critical, and we stipulate that *IHV* should only be used with its ordinary meaning for stations that are equatorward of 55°. A similar stipulation holds for the well-known *K* index. In fact, the strong dependence on latitude above 55° might possibly afford a means to monitor the long-term variation of the position of the auroral zone.
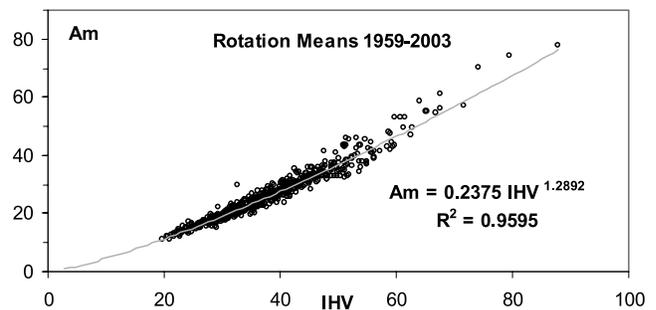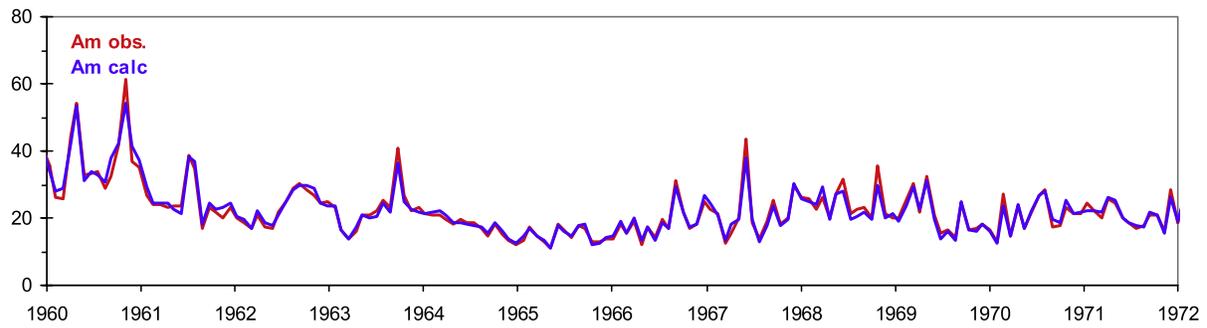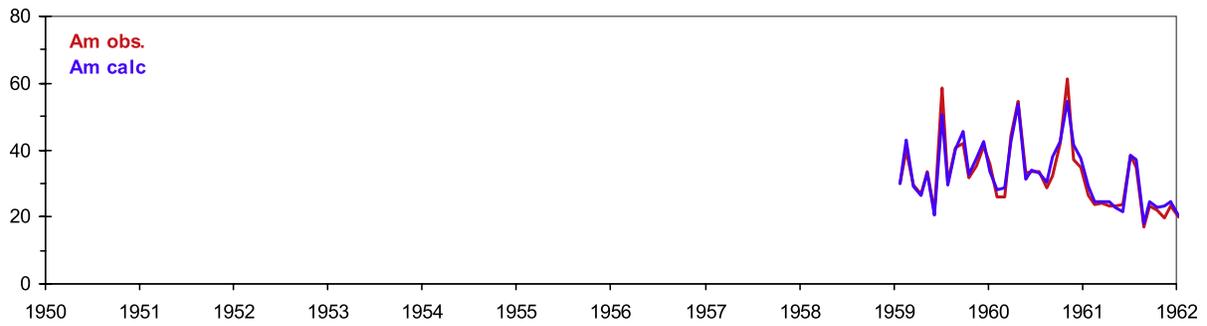

Figure 8. Relationship between Bartels rotation means of *Am* (freed for dipole tilt effect) and composite *IHV* for the interval 1959–2003.
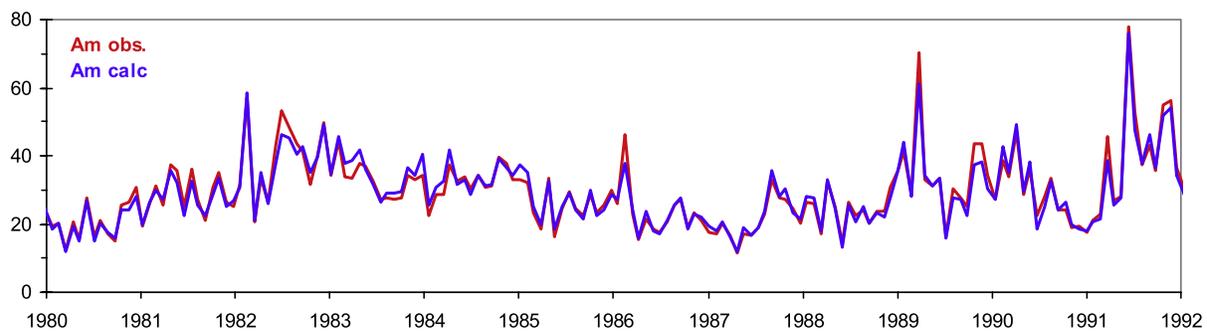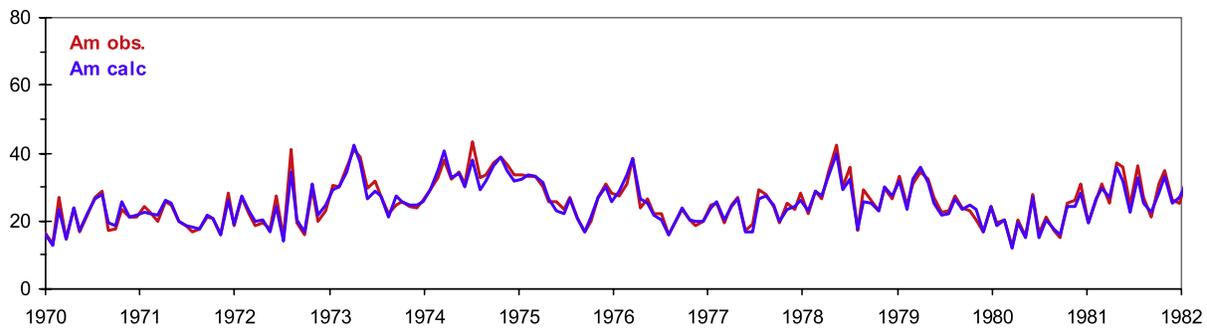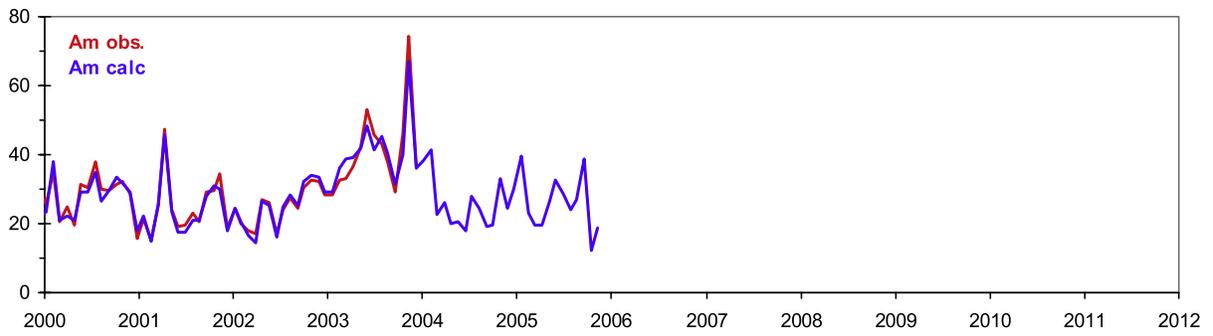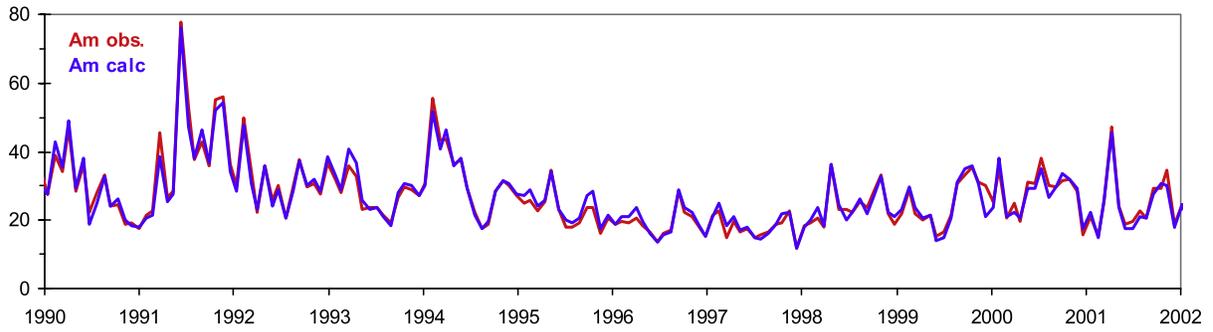
a.

b.

Figure 9. (top) Bartels rotation averages of proxy values of *Am* calculated using equation (4) (blue curve) and observed (red curve). Both data sets have been freed from the effect of the dipole tilt (section 3.2). Also shown are (bottom) the entire data sets overlain by their 13-rotation running means.
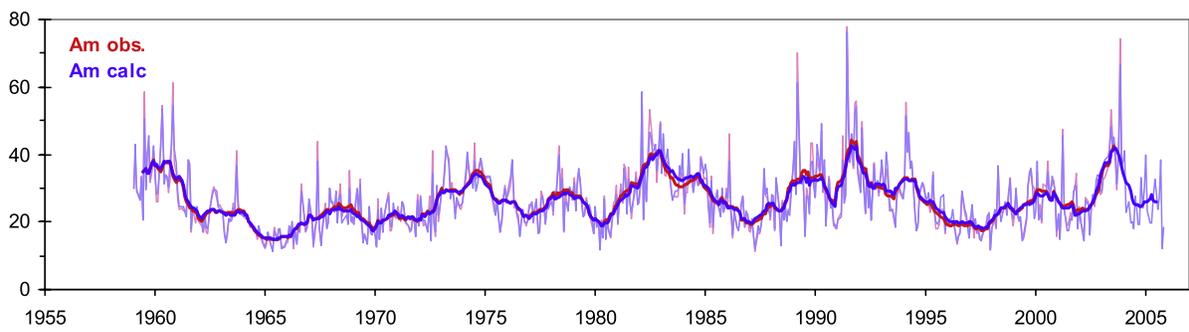
c.

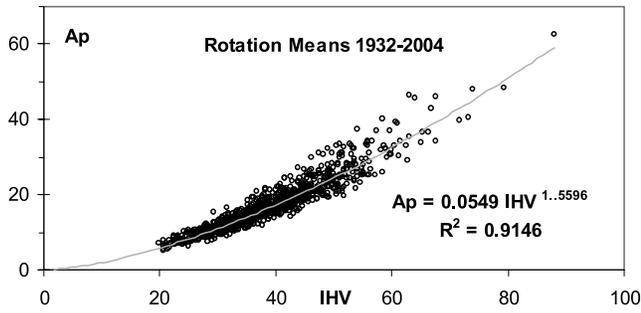

d.

Figure 9b.   (continued)

Figure 10. Relationship between Bartels rotation means of *Ap* (freed for dipole tilt effect) and composite *IHV* for the interval 1932–2004.
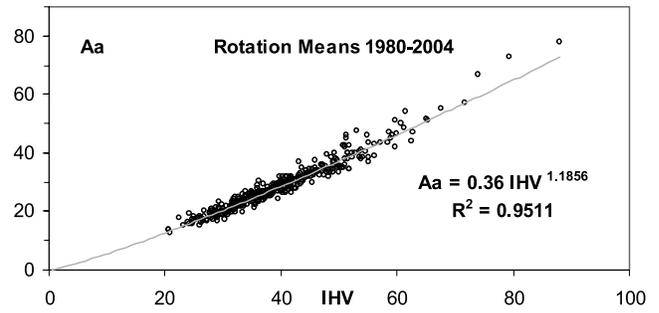

Figure 12. Relationship between Bartels rotation means of *Aa* (freed for dipole tilt effect) and composite *IHV* for the interval 1980–2004.

[21] Also shown in Figure 5 is a fit to the data points by a simple ad hoc model consisting of the sum of four Gaussian functions, namely,

$$IHV(\varphi) = \sum_k \left[a_k \exp\left\{ -b_k [\text{abs}(\sin(\varphi)) - \sin(\varphi_k)]^2 \right\} \right] \quad (3)$$

where a_k ($k = 1, \ldots, 4$) define the scale (relative to a station at $\varphi = 48°$ (i.e., NGK) with $\langle IHV \rangle = 34.33$ for 1996–2003), b_k is the width, and φ_k is the position of the peaks. These parameters are given in Table 2. The values of φ_k were prescribed except for $k = 3$, which represents a least squares fit. The model is descriptive only and does not pretend much physical content with the exception of the identifica-

tion of the auroral zone peak. As illustrative of the sensitivity of *IHV* to the location of the auroral zone, we note that a change of three degrees of either φ or φ_3 entails a change of *IHV* by a factor of two for φ near $60°$.

3.4. Cautionary Notes and Technical Details

[22] In the course of developing the *IHV* index, we encountered a number of technical issues and concerns related to the data used. These are covered in detail in Appendix A. Although relegated to an appendix, these issues are of utmost importance and must be dealt with properly. They include: (1) nonremoval of "residual" regular variation; (2) use of hourly values instead of hourly means in older data; (3) effect of extreme activity; (4) station specific artifacts in archival data; (5) the effect of secularly

Figure 11. (top) Sample Bartels rotation averages of proxy values of *Ap* calculated using equation (5) (blue curve) and observed (red curve). Both data sets have been freed from the effect of the dipole tilt (section 3.2). (bottom) Shows the entire data sets overlain by their 13-rotation running means.
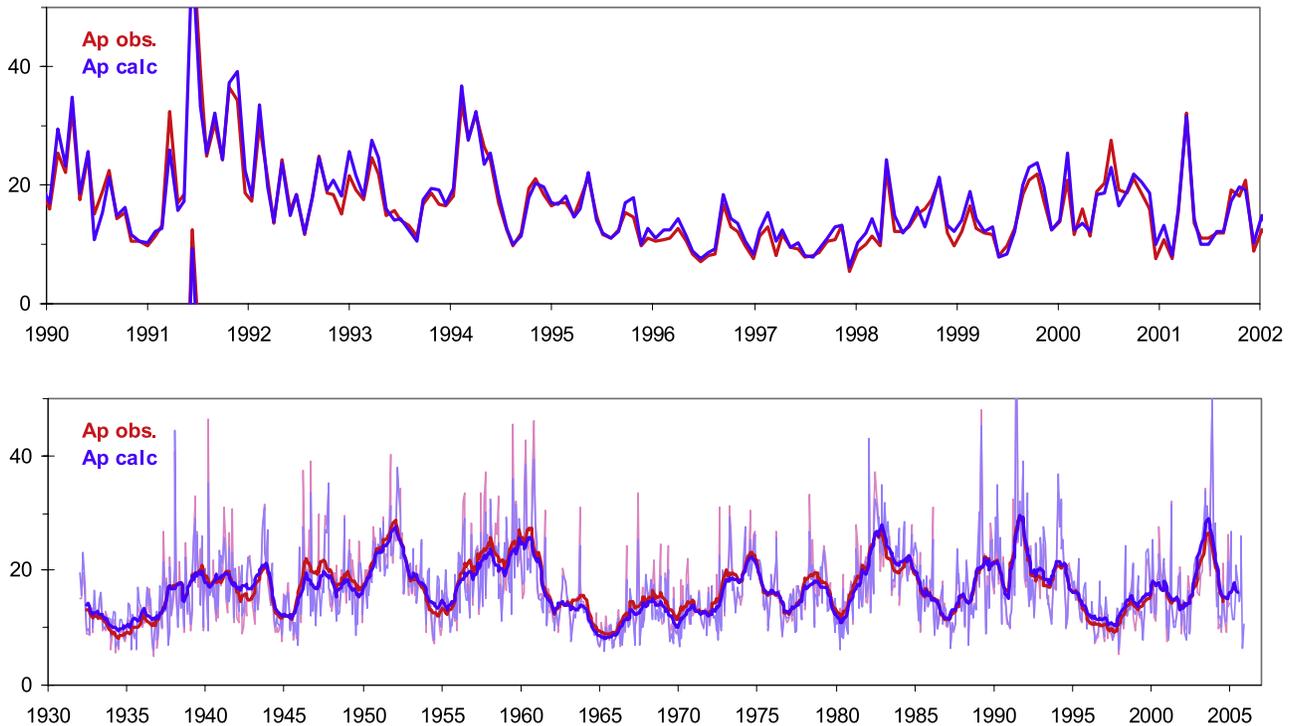
Figure 13. (top) Sample Bartels rotation averages of proxy values of *Aa* calculated using equation (6) (blue curve) and observed (red curve). Both data sets have been freed from the effect of the dipole tilt (section 3.2). (bottom) Shows the entire datasets overlain by their 13-rotation running means.
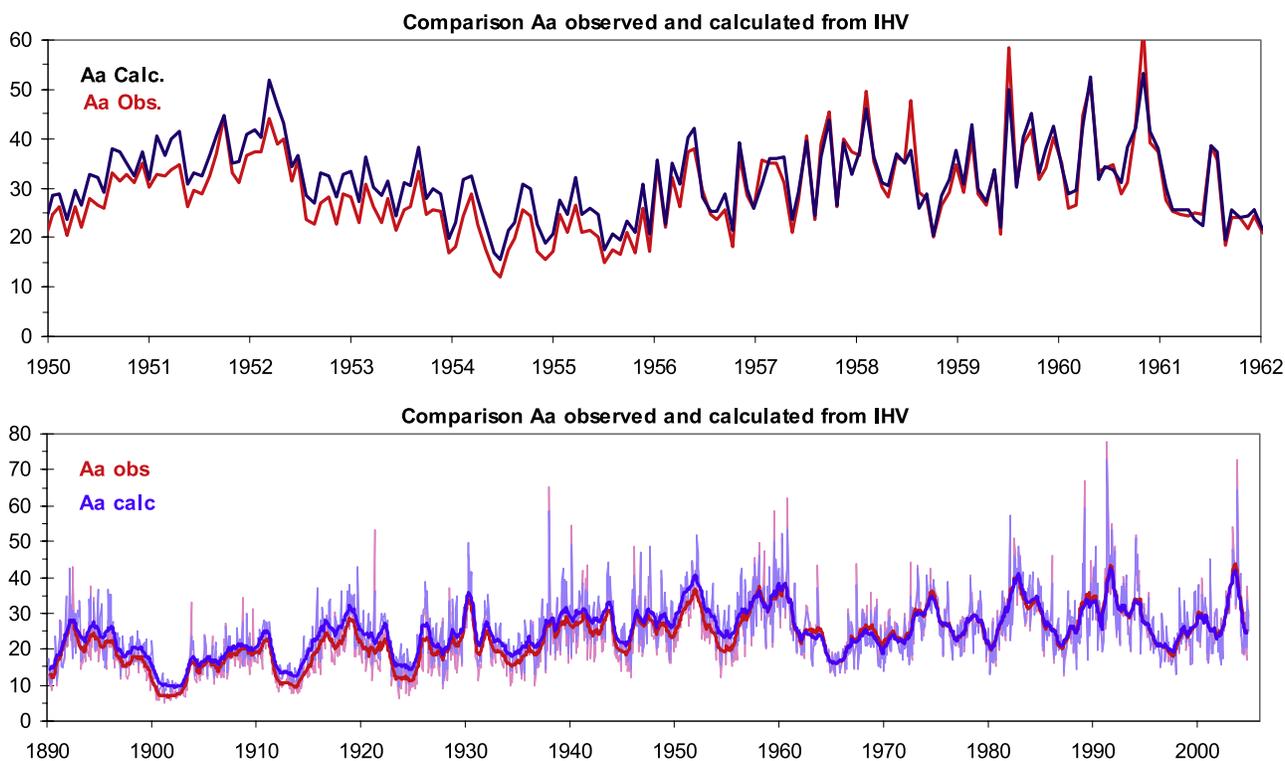
changing geomagnetic dipole position and strength; (6) missing data during severe storms; (7) possible seasonal bias.

3.5. Longitude Sectors, Hemispheric Series, and Equatorial Series

[23] Although the geographic distribution of geomagnetic observatories suffers from the usual deficiencies of coverage over oceans and in the Southern Hemisphere, we have found it possible to construct long time series of *IHV* for the six longitude sectors described in section 3.3. In each sector we define *IHV* series separately for the two hemispheres yielding a total of 12 independent *IHV* series with various degrees of time coverage. In addition, we construct a series using stations close to the geomagnetic equator (within 9°). For the purpose of comparing and normalizing *IHV* for different stations, the series are calculated as averages over Bartels rotations (with at least 20 days of data). Figures S1 through S12 in the auxiliary material shows the *IHV* series for each station within each longitude sector.[1]

[24] The longest of all series is constructed from the German stations Potsdam (POT: 1890–1907), Seddin (SED: 1908–1931), and Niemegk (NGK: 1932–present), supplemented with data from Wilhelmhafen (WLH: 1883–1895). This series of superb observations serves as a "reference" series, all other series being calibrated and normalized to the WLH-POT-SED-NGK series. The normalization is necessary because of different underground electrical conductivity or seawater "coast" effects. These effects often exceed the small effect of differing latitudes so we have adopted the practice of not having a separate latitude effect on top of the overall normalization factors, avoiding *Mayaud*'s [1973, p.7] mistake of correcting twice for latitude.

4. Calibration of Longitude Sectors and a Global Index

4.1. Calibration of Single Sectors: Principle of Overlap

[25] Within each sector we select stations such that there is maximal overlap in time. Two stations that have data that do not overlap can be compared if a third station, or better, as is often the case, several stations, overlap with the stations to be compared such as to form one or more "bridges." For overlapping data we perform a linear regression analysis. Figure 6 shows a typical example. Rare outliers (one is marked by the large open circle) are identified and are not included in calculating the linear slope (or "scale") between the two stations. The "offset" is usually small to insignificant, so we force the offset to zero. The square of the linear correlation coefficient (R^2) indicates how good the fit is. Because both of the data sets that are being correlated have errors or variance not accounted for by the correlation, the "usual" method (that minimizes the sum of the squares of the ordinate deviations) is not applicable. The "proper" way of dealing with this problem

---

[1]Auxiliary material data sets are available at ftp://ftp.agu.org/apend/ja/2007ja012437. Other auxiliary material files are in the HTML.
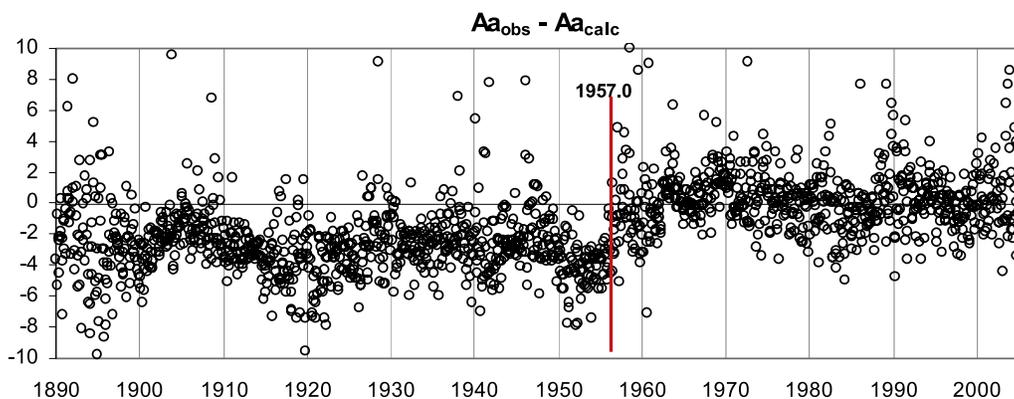
Figure 14. Difference between observed and calculated values of Bartels rotation means of *Aa* showing the upward jump in 1957.

has a 100-year literature [e.g., *Parish*, 1989]. We use a method equivalent to minimizing the sum of the squares of the perpendicular distances along both axes to the best fit line, rather than just the vertical distances. The correlations are usually good enough that the problems associated with "constrained" regression are not a concern (e.g., in calculating R^2). The data has heteroscedacity (larger values scatter more than smaller values), but this is mostly offset by larger values being progressively rarer. In reporting slopes, we shall quote four decimals throughout, being sufficiently (even overly) precise that rounding errors are avoided. In Appendix B we detail the construction and calibration of each sector.

[26] An overriding principle has been to avoid hidden empirical adjustments, and in cases where normalizations were used, to make these reversible and transparent. Anyone should be able to recalculate the index from public archival data. As more data become available, index values may change slightly. There will thus not be a definitive "official" version of a "global" *IHV* index. In this we recognize the importance of future recalibration (by anybody) based on improved data and understanding. We propose that a given version of *IHV* be annotated with the year of its release, e.g., *IHV2007* for the version derived in the present paper.

4.2. Composite *IHV* Series

[27] A composite *IHV* series can be formed by first adding the average *IHV* values for all of the longitudinal sectors that have data for each Bartels rotation. To compensate for the fact that data may be missing for certain sectors from time to time, the summed *IHV* for each rotation is divided by the number of sectors that contributed data for that rotation, effectively calculating the mean with each sector having the same weight. The composite *IHV* now becomes a true daily index: successive longitude sectors contributing their 6-hour slices as the Earth turns. The variation from sector to sector is simply the variation of geomagnetic activity with time. Because geomagnetic activity has a high degree of conservation, the *IHV* index for one sector is strongly correlated with the *IHV* index for the following sector(s). It is this property that makes it possible to normalize all sectors to the Northern Hemisphere part of the sector centered on longitude 15° (called IHV15N,

effectively to NGK) with the scaling factors given in Table 3. Since all sectors are ultimately reduced to NGK, any intrinsic variation (apart from that related to the dipole tilt, see section 3.2) of geomagnetic activity with longitude or with hemisphere is not reflected in the *IHV* series.

[28] The top of Figure 7 shows a portion of the individual data series that went into the composite series. Northern sectors are shown in black while southern sectors are shown in red. A rotation by rotation plot of the full series is shown in Figure S14 of the auxiliary material. The middle of Figure 7 shows the full series overlain by its 13-rotation running mean. The bottom of Figure 7 shows 13-rotation running means of the composite *IHV* (blue) and *IHV* derived from equatorial stations (red). The entire composite data set is given in Table T1 of the auxiliary material.

4.3. No Seasonal Variation of the *IHV* Index

[29] We can also construct composite *IHV* series for each hemisphere separately. Because of the normalization of each sector to IHV15N there will be no general difference in activity level between hemispheres, but it is of interest to investigate the variation of the index with time (annual phase) of year since one of the rationales for constructing indices based on the mean of antipodal observations (such as *aa*) is to cancel out any variation tied to the seasons. We show in Appendix A.7 that there does not seem to be any significant seasonal variation, i.e., related to summer/winter differences. This is important for construction of a global index (usable for inferring solar properties) from *IHV* when we only have data for one hemisphere (at the time of writing
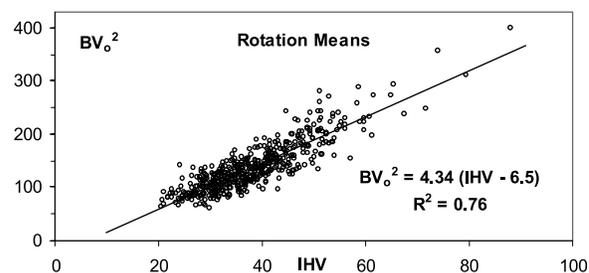

Figure 15. Relationship between Bartels rotation means of $BV_o{}^2$ and composite *IHV* for the interval 1965–2005.
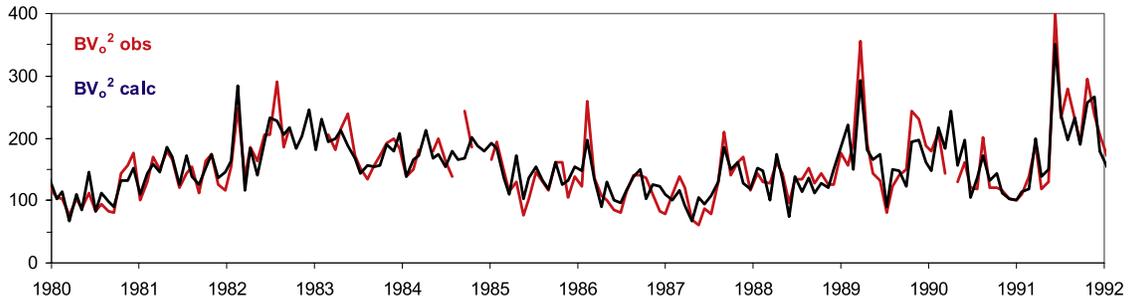
Figure 16. Sample Bartels rotation averages of proxy values of BV_o^2 calculated using equation (7) (blue curve) and observed (red curve).

there is very little Southern Hemisphere data before 1915, see Table 3). With no seasonal (i.e., summer/winter) variation such missing data is not going to skew the result in any systematic or appreciable way.

5. Comparison With Geomagnetic Range Indices

[30] In this section we compare the composite *IHV* series with the family of range indices comprising the *am*, *ap*, and *aa* indices with emphasis on long-term stability. The composite *IHV* index is derived from many longitudinal sectors in each hemisphere comprising many stations with much overlap of data. The excellent agreement between all these independent series is interpreted as confirmation of the long-term stability of the composite *IHV* index. The auxiliary material contains detailed, rotation by rotation comparison plots (Figures S15 and S16).

5.1. Comparison With the *am* Index

[31] Figure 8 shows the relationship between rotation means of (composite) *IHV* and the *am* index. As with *IHV*, we have removed the dipole tilt-related variations by dividing *am* by the S function (equation (2)). The clearly nonlinear relation can be expressed as:

$$Am = 0.2375 \ IHV^{1.2892}, \quad (R^2 = 0.96) \qquad (4)$$

R^2 is calculated from the linear relationship between the logarithms. The excellent (near perfect) fit means that we can use *IHV* as a proxy for *Am* (and similar range indices). Figure 9 shows the *Am* proxy calculated from *IHV* using equation (4) in extenso for every Bartels rotation where we

have data. The *am* index is probably the best range index available at this time, based as it is on a satisfactory station distribution. We urge the reader to study this compelling figure.

5.2. Comparison With the *ap* Index

[32] Figure 10 shows the relationship between rotation means of (composite) *IHV* and the *ap* index. As with *IHV*, we have removed the dipole tilt-related annual and UT variations by dividing *ap* by the S function (equation (2)). Because the UT variation was deliberately sought eliminated when the *Kp* index tables were drawn up [*Bartels et al.*, 1939], one might try to evaluate the S function with UT set to a constant value (say 12) for every 3-hour interval during the day. This, however, results in a markedly lower correlation ($R^2 = 0.85$), so we resort to using the actual UT. The clearly nonlinear relation can be expressed as:

$$Ap = 0.0549 \ IHV^{1.5596}, \quad (R^2 = 0.91) \qquad (5)$$

The correlation is significantly worse than for the *am* index, reflecting the high quality of the *am* index. Figure 11 shows the *Ap* proxy calculated from *IHV* using equation (5). Inspection of Figure 11 shows that there is no systematic drift between the observed and calculated values of *Ap* over the entire interval 1932–2004. For no 10-year interval does the absolute difference between the observed and calculated averages of *Ap* exceed 5%. This means that we can use *IHV* as a stable proxy for *Ap*. There are, however, from time to time for intervals of a few years, systematic differences showing that *Ap* is not quite homogenous.
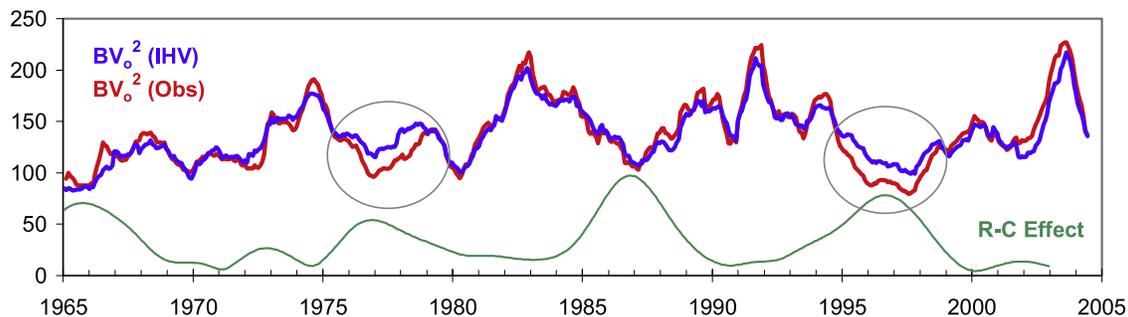

Figure 17. The 13-rotation running means of BV_o^2, calculated (blue curve) and observed (red curve). Areas of consistent disagreement are marked by ovals. These occur every other time when the Rosenberg-Coleman effect is large (amplitude on arbitrary scale given by green curve).
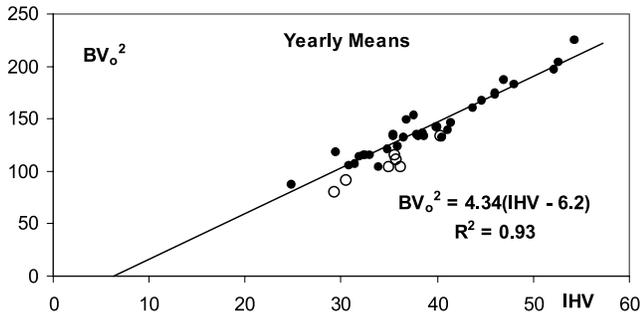
Figure 18. Relationship between yearly means of BV_o^2 and composite *IHV* for the interval 1965–2005. Years affected by the 22-year cycle are shown as open circles and are not included in the fit.

5.3. Comparison With the *aa* Index

[33] Figure 12 shows the relationship between rotation means of (composite) *IHV* and the *aa* index for the time interval (1980–2004) since the latest (published) change of the *aa* calibration table values. As with *IHV*, we have removed the dipole tilt-related annual and UT variations by dividing *aa* by the *S* function (equation (2)). The clearly nonlinear relation can be expressed as:

$$Aa = 0.3600 \ IHV^{1.1856}, \quad (R^2 = 0.95) \qquad (6)$$

The excellent fit (almost as good as for *Am*) means that we should be able to use *IHV* as a proxy for *Aa* as well. Figure 13 shows the *Aa* proxy calculated from *IHV* using equation (6).

[34] As Figure 13 shows, the observed values of *Aa* match the calculated proxy values very well back in time until about the beginning of 1957. Before that time, observed *Aa* is consistently smaller than calculated *Aa*. Figure 14 shows the difference in a more compact format. The jump at 1957.0 is 2.9 nT or 12% of the average value of *Aa*. At times where *Aa* is much smaller, such as at the beginning of the 20th century, the percentage discrepancy is much larger (~40%). We interpret the difference to be an indication that the calibration of *aa* as measured by rotational means before 1957 is in error by this amount. A

similar conclusion was already reached by *Svalgaard et al.* [2003, 2004], *Jarvis* [2005], *Mursula and Martini* [2006], and Lockwood et al. (submitted manuscript, 2007). A critical reexamination and recalibration of the *aa* index will be covered in a subsequent paper in this series. It would seem that *IHV* could serve as a useful tool for checking the stability of geomagnetic indices, both for past values and for ongoing quality control. That such ongoing control is needed should be clear from the account by *Lincoln* [1977] in the work of *van Sabben* [1977].

6. Comparison With External Solar Wind Drivers

[35] The earliest solar wind data showed strikingly that geomagnetic activity depends strongly on solar wind speed [*Snyder et al.*, 1963]. It is well-established [e.g., *Svalgaard*, 1977; *Murayama and Hakamada*, 1975; *Lundstedt*, 1984] that geomagnetic range indices (such as *am*) are robustly correlated with $P = q \ BV^2$, where *B* is the magnitude of the interplanetary magnetic field impinging on the Earth with solar wind speed *V*. The geometric factor *q* parameterizes the effect of magnetic merging depending on the angle (and of its variability over the 3-hour interval) between interplanetary and terrestrial magnetic fields. We shall initially assume that the average *q* over a rotation does not vary from one Bartels rotation to the next. We also ignore a very weak dependence of solar wind density *n*, in the form $n^{1/3}$ [*Svalgaard*, 1977]. We show in section 6.2 that the *IHV* index is a sensitive indicator of *P*, responding directly and simply to this external solar wind driver.

6.1. Solar Wind Data

[36] In situ near-Earth solar wind data is available from the OMNIWEB Web site at http://www.omniweb.org. We utilize Bartels rotation averages of *B* and *V*. First, daily averages are calculated from hourly averages. If there is any data at all for a given day, its daily average goes into the rotation average. If the rotation average is based on less than 20 days of daily averages, the rotation is not used. For some years (especially during the 1980s) there were significant amounts of data missing. Over a timescale of 27 days and longer there is little difference between $\langle B \rangle \langle V \rangle^2$ and $\langle BV \rangle$. We use the separable version, $\langle B \rangle \langle V \rangle^2$, because our

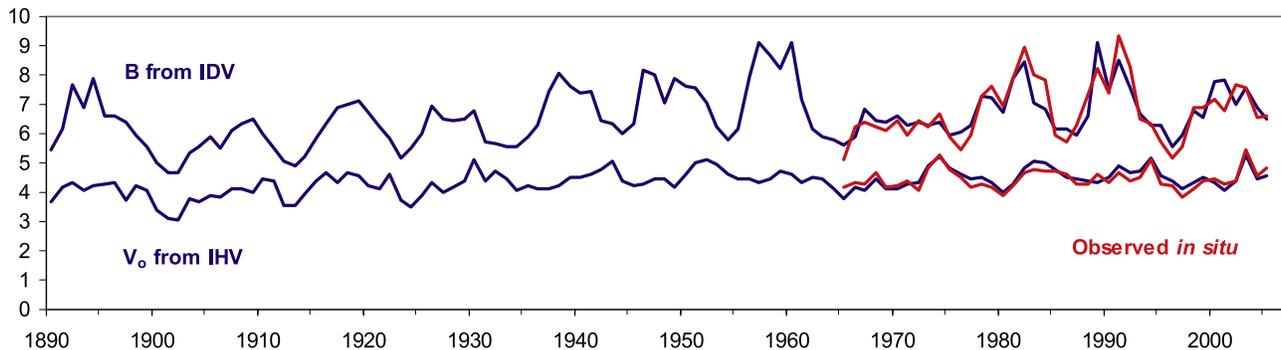**Figure 19.** Yearly values of *B* (nT) derived from the *IDV* index (equation (10), upper blue curve) and *V* calculated using equation (11) (lower blue curve). *V* is plotted as $V_o = V/100$ km/s. *B* and *V* observed in space are shown in red.

Table 4. Yearly Values of Composite *IHV, B* Derived From the *IDV* Index, *V* Calculated Using Equation (11), and *B* and *V* Observed by Spacecraft[a]

Year	IHV	B_{IDV}	B_{obs}	V_{calc}	V_{obs}
1890.5	23.01	5.47		365	
1891.5	31.13	6.15		419	
1892.5	39.15	7.69		431	
1893.5	32.35	6.90		406	
1894.5	38.47	7.92		421	
1895.5	33.99	6.59		428	
1896.5	34.56	6.62		431	
1897.5	26.74	6.37		374	
1898.5	30.53	5.93		422	
1899.5	26.97	5.54		403	
1900.5	19.63	5.02		341	
1901.5	16.65	4.66		312	
1902.5	16.13	4.69		303	
1903.5	23.62	5.34		376	
1904.5	23.59	5.53		369	
1905.5	26.54	5.88		388	
1906.5	25.16	5.52		386	
1907.5	29.89	6.11		410	
1908.5	30.67	6.34		409	
1909.5	29.93	6.50		398	
1910.5	33.64	6.00		446	
1911.5	30.37	5.48		438	
1912.5	21.12	5.08		357	
1913.5	20.46	4.87		356	
1914.5	24.78	5.21		393	
1915.5	31.87	5.82		438	
1916.5	37.97	6.34		466	
1917.5	35.84	6.90		432	
1918.5	40.92	6.97		465	
1919.5	40.12	7.09		456	
1920.5	33.86	6.73		422	
1921.5	30.58	6.24		412	
1922.5	34.95	5.85		462	
1923.5	22.60	5.18		371	
1924.5	22.03	5.53		353	
1925.5	26.97	6.00		388	
1926.5	36.03	6.95		432	
1927.5	29.99	6.49		399	
1928.5	31.74	6.43		415	
1929.5	34.93	6.52		437	
1930.5	47.20	6.77		513	
1931.5	31.56	5.72		439	
1932.5	35.15	5.67		471	
1933.5	31.48	5.53		445	
1934.5	27.13	5.53		405	
1935.5	30.42	5.87		423	
1936.5	30.45	6.29		409	
1937.5	34.84	7.43		409	
1938.5	39.21	8.08		421	
1939.5	42.07	7.61		452	
1940.5	40.31	7.39		447	
1941.5	42.41	7.45		459	
1942.5	39.82	6.46		475	
1943.5	43.67	6.32		507	
1944.5	32.66	6.03		437	
1945.5	32.12	6.34		421	
1946.5	41.06	8.19		430	
1947.5	42.11	7.98		442	
1948.5	38.57	7.03		447	
1949.5	37.98	7.87		419	
1950.5	43.28	7.59		460	
1951.5	49.66	7.54		500	
1952.5	49.00	7.04		514	
1953.5	41.28	6.23		494	
1954.5	34.38	5.78		460	
1955.5	34.52	6.19		446	
1956.5	42.18	7.93		444	
1957.5	45.34	9.11		432	
1958.5	45.23	8.66		442	
1959.5	48.11	8.21		471	

Table 4. (continued)

Year	IHV	B_{IDV}	B_{obs}	V_{calc}	V_{obs}
1960.5	50.59	9.09		460	
1961.5	37.60	7.18		436	
1962.5	34.92	6.14		451	
1963.5	33.04	5.91		444	
1964.5	28.63	5.76		411	362
1965.5	24.79	5.60	5.09	380	415
1966.5	29.42	5.87	6.20	415	436
1967.5	32.25	6.86	6.38	406	426
1968.5	35.34	6.42	6.24	444	464
1969.5	31.28	6.40	6.09	412	418
1970.5	31.93	6.59	6.44	412	420
1971.5	32.48	6.26	5.97	427	439
1972.5	33.80	6.40	6.43	433	403
1973.5	41.24	6.31	6.21	491	485
1974.5	46.78	6.40	6.66	525	531
1975.5	38.38	5.93	5.90	485	480
1976.5	35.66	6.04	5.42	460	451
1977.5	34.82	6.28	5.96	445	418
1978.5	40.10	7.29	7.27	449	429
1979.5	37.82	7.24	7.59	435	418
1980.5	30.65	6.71	6.96	398	389
1981.5	39.91	7.90	7.87	430	424
1982.5	51.99	8.46	8.93	485	469
1983.5	47.95	7.07	8.01	506	477
1984.5	45.87	6.81	7.81	503	471
1985.5	38.72	6.19	5.95	478	472
1986.5	34.86	6.14	5.74	450	459
1987.5	32.97	5.93	6.26	442	428
1988.5	35.47	6.62	7.31	438	428
1989.5	46.07	9.12	8.20	436	460
1990.5	41.09	7.51	7.39	449	434
1991.5	52.63	8.52	9.35	486	467
1992.5	43.68	7.53	8.26	465	440
1993.5	40.60	6.68	6.52	473	451
1994.5	44.60	6.30	6.35	514	514
1995.5	36.24	6.30	5.72	455	426
1996.5	30.56	5.56	5.18	436	421
1997.5	29.32	5.93	5.54	411	381
1998.5	35.62	6.78	6.89	434	409
1999.5	36.54	6.56	6.87	448	439
2000.5	39.87	7.80	7.14	433	446
2001.5	35.86	7.84	6.80	405	427
2002.5	36.93	6.97	7.69	437	439
2003.5	54.28	7.53	7.54	526	545
2004.5	37.90	6.90	6.55	447	453
2005.5	37.63	6.50	6.22	458	473
2006.5	*27.84*	*5.2*	*5.07*	*411*	*429*
2007.3	*28*	*5.0*	*4.7*	*430*	*440*

[a]*B* in nT and *V* in km/s. Values for 2006 and 2007 are preliminary only, based on incomplete data.

ultimate goal is to calculate $\langle V \rangle$. We shall often use the abbreviation V_o for the quantity $V/(100 \text{ km/s})$. When we calculate regression lines involving interplanetary parameters we have treated those as dependent variables with errors (e.g., caused by missing data) assuming *IHV* to be "error free." This is guided by our wish to see how well we can estimate BV_o^2 from *IHV* and not how well we can calculate *IHV* from BV_o^2 (see the exchange in the work of *Lockwood et al.* [2006] and *Svalgaard and Cliver* [2006]). Available interplanetary data are for several years only poorly representative of true solar wind conditions because of significant amounts of missing data (approaching 60% or more during 1983–1994).
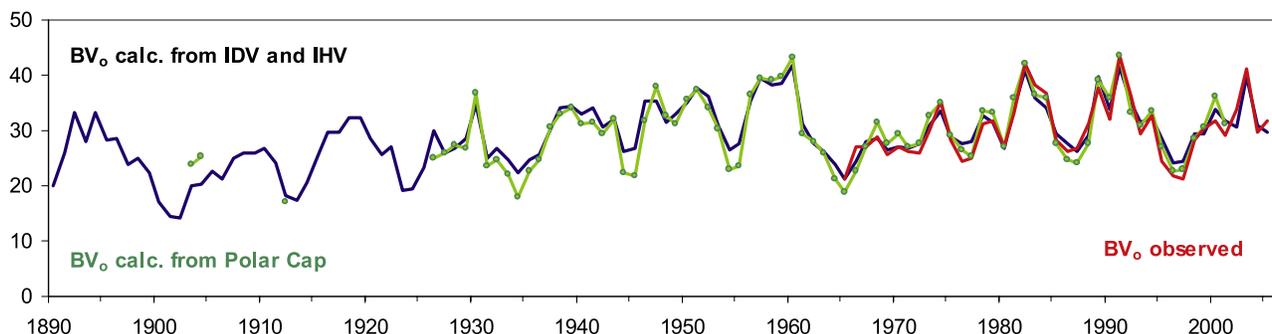
Figure 20. Yearly values of BV_o (blue curve) calculated from B derived from the *IDV* index (equation (10)) and V derived from the IHV index (equation (11)) compared to BV_o (green curve) calculated from the range of diurnal variation of the horizontal component in the polar caps. BV_o calculated from B and V observed in space is shown in red.

6.2. *IHV* Dependence on BV^2 (Rotation Timescale)

[37] Figure 15 shows the correlation between the composite **IHV** series and BV_o^2. Assuming the simple linear form suggested by Figure 15, the relationship can be written:

$$BV_o^2 = (4.33 \pm 0.11)(IHV - 6.4 \pm 1.0), \quad R^2 = 0.77 \quad (7)$$

Figure 16 shows how well *IHV* reproduces BV_o^2. There is detailed agreement even on a timescale as short as one rotation.

[38] Figure 17 shows 13-rotation (∼1 year) running means of calculated BV_o^2 and observed values of BV_o^2 back to 1965. Close examination shows systematic disagreements concentrated in certain years: 1975–1978 and 1995–1998. It is no coincidence that these intervals are ∼22 years apart. The Russell-McPherron effect [*Russell and McPherron*, 1973] gives rise to a semiannual variation of geomagnetic activity that usually is very small, except when the Rosenberg-Coleman effect [*Rosenberg and Coleman*,

1969; *Wilcox and Scherrer*, 1972] is pronounced. *Echer and Svalgaard* [2004] found that the Rosenberg-Coleman effect tends to occur only near sunspot minimum and then for a few years thereafter during the rising phase of the solar cycle as shown in Figure 17 by the amplitude of the R-C effect determined by wavelet analysis. The R-M effect plus a strong, short-lived R-C effect combined with a reversal of the large-scale solar polar fields gives rise to a few years of enhanced geomagnetic activity every ∼22 years [*Chernosky*, 1966; *Russell and Mulligan*, 1995; *Cliver et al.* 1996] that will result in *IHV* being larger than usual during such times. The two short periods of (minor) disagreements between the observed and calculated values of BV_o^2 were just two such times. Another one (and an extreme one at that) was the year 1954 [*Cliver et al.*, 2004] and some disagreements would be expected around 1934–1935, 1913–1915, 1890–1892, etc.
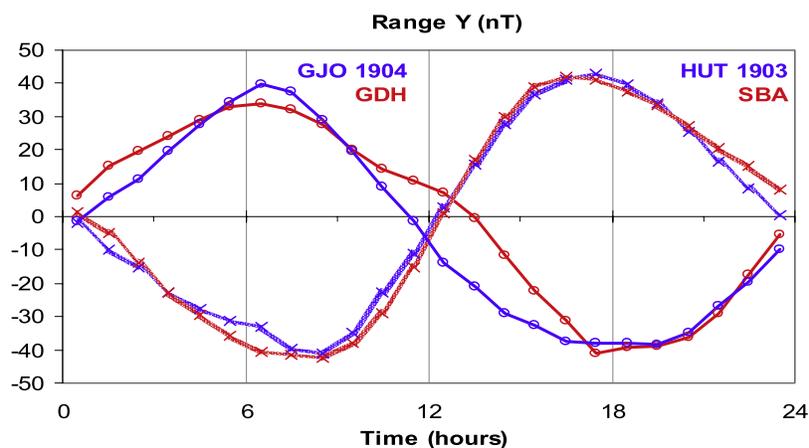

Figure 21. The diurnal variation of the Y-component of the geomagnetic field at SBA (red, crosses), HUT (blue crosses; for 1902.5–1903.5), GJO (blue circles; for 1904), and GDH (red circles) all in a local coordinate system where the X axis coincides with the average direction of the H component. The curves have been shifted in time to have the same phase in each hemisphere but out of phase between hemispheres. This is simply a presentation device to avoid having the curves crowd on top of each other. For SBA and GDH, modern data was used for years with approximately the same sunspot activity as during 1903–1904 as described in the text.

Table 5. Range of Polar Cap Diurnal Variation of the Horizontal (Y) Component for the Stations Given (With Their IAGA Station Designations)[a]

Station	IAGA	Year	$\langle R_z \rangle$	CGMlat	ΔY nT	$\Delta Y'$ nT	BV	V	B	B_{IDV}
Winter Quarters	HUT	1903.0	14	$-81.2°$	83.9	*78.4*	*2316*	*446*	*5.19*	5.02
Gjøahavn	GJO	1904.5	42	79.3°	78.1	*71.1*	*2427*	*414*	*5.86*	5.53
Scott Base	SBA	>1964	14.4	$-79.9°$	84.4	84.4	*2493*	*446*	*5.71*	5.94
Qeqertarsuaq	GDH	>1964	37.9	77.0°	75.0	75.0	*2560*	*414*	*6.17*	6.16

[a]The product *BV* is derived from the range. See text for column details.

[39] If the few years of 22-year cycle "contamination" are not included in the fit, the relationship between BV_o^2 and *IHV* becomes

$$BV_o^2 = (4.25 \pm 0.11)(IHV - 5.0 \pm 0.9), \quad R^2 = 0.79 \quad (8)$$

The smallest values of *IHV* averaged over a rotation in the ~120-year series are around 13 (only 5 values out of more than 1600 are smaller than 14). By way of illustration, *IHV* ~13 gives BV_o^2 ~34 which would be satisfied by $B = 4.5$ nT and $V = 275$ km/s.

[40] The excellent agreement between observed and calculated values of BV_o^2 even before 1974 suggests that the interplanetary measurements are of high quality and that

one cannot maintain that the accuracy of the IMF and solar wind data was low during the "baby" period of the space age [e.g., *Stozhkov and Pokrevsky*, 2001] as a reason for differences between inferred and observed parameters.

6.3. *IHV* Dependence on BV^2 (Yearly Timescale)

[41] We compute the yearly mean of *IHV* (or of BV_o^2) for a given year by averaging over Bartels rotations spanned by the year. Figure 18 shows the relationship between yearly means of BV_o^2 and *IHV*. Omitting the few years of 22-year enhancements yields this regression equation for yearly means:

$$\langle B \rangle \langle V_o \rangle^2 = (4.34 \pm 0.21)(\langle IHV \rangle - 6.2 \pm 1.9), \quad R^2 = 0.93 \quad (9)$$

Table 6. Geomagnetic Observatories With Long Series of Data That May Be Useful for Constructing *IHV* Indices[a]

Long. Lat	Name	From-To	Name	From-To	Name	From-To
0E 41N	Ebro	1910-...				
3E 48N	Saint Maur	1883–1900	Val Joyeux	1901–1936	Chambon la Forêt	1936-...
5E 50N	Uccle	1896–1919	Manhay	1936–1971	Dourbes	1955-...
6E 52N	Utrecht	1891–1896	De Bilt	1899–1938	Witteveen	1938–1988
8E 54N	Wilhelmshafen	1883–1911	Wingst	1939-...		
11E 60N	Oslo	1843–1930				
13E 52N	Potsdam	1890–1907	Seddin	1908–1931	Niemegk	1932-...
13E 57N	Copenhagen	1891–1908	Rude Skov	1907–1978	Brorfelde	1978-...
25E 60N	Helsinki	1844–1897	Nurmijärvi	1953-...		
31E 30N	Helwan	1903–1959	Missalat	1960-...		
31E 60N	St. Petersburg	1869–1877	Slutsk	1878–1941	Voeikovo	1947-...
45E 42N	Tiflis	1879–1905	Karsani	1905–1934	Dusheti	1938-...
48E 19S	Antananarivo	1890-...				
49E 56N	Kazan	1892–1913				
58E 20S	Mauritius	1892–1965				
61E 57N	Sverdlovsk	1887–1978	Vysokaya-Dubrava	1932-...		
73E 19N	Colaba	1846–1905	Alibag	1904-...		
77E 10N	Kodaikanal	1902-...				
107E 6S	Batavia	1867–1944	Kuyper	1950–1962	Tangerang	1964-...
114E 22N	Hong Kong	1884–1928	Au Tau	1928–1939	Hong Kong	1972-...
121E 15N	Manila	1891–1904	Antipolo	1910–1938	Muntinlupa	1951-...
121E 31N	Zi-Ka-Wei	1875–1907	Lukiapang	1908–1933	Zo-Se	1933–1974
145E 38S	Melbourne	1865–1921	Toolangui	1922–1980	Canberra	1980-...
173E 43S	Amberley	1929–1977	Lauder	1977–1978	Eyrewell	1979-...
188E 14S	Apia	1905-...				
261E 20N	Teoloyucan	1923-...				
281E 44N	Agincourt	1881–1969	Ottawa	1968-...		
294E 22S	La Quiaca	1920-...				
296E 32S	Pilar	1905-...				
316E 22S	Vassouras	1915-...				
334E 38N	Sao Miguel	1911-...				
352E 40N	Coimbra	1866-...				
356E 36N	San Fernando	1891-...				
358E 54N	Stonyhurst	1865–1967				
360E 51N	Greenwich	1846–1925	Abinger	1925–1957	Hartland	1957-...
360E 51N	Kew	1858–1924				

[a]If a station stopped observing, the next column(s) may give the replacement station(s) (if any). For many stations there are data even earlier than given here, e.g., Paris and Munich. The coordinates given in the first column are geographic longitude and latitude.

We may note that all the regression equations (7) through (9) are identical within their statistical errors.

6.4. Determination of Solar Wind Speed

[42] In the work of *Svalgaard and Cliver* [2005] we showed how yearly averages of B could be determined from our *IDV* index:

$$\langle B \rangle = (3.04 \pm 0.37) + (0.361 \pm 0.035)\langle IDV \rangle, \quad R^2 = 0.74 \tag{10}$$

Combining equations (9) and (10) yields

$$\langle V \rangle = 347 \text{ km/s}[(\langle IHV \rangle - 6.20)/(\langle IDV \rangle + 8.42)]^{1/2}, \tag{11}$$

allowing determination of V from *IHV* and *IDV*. Figure 19 shows B and V_o since 1890. Over the ~120-year series, the solar wind speed varied from a low (inferred) value of 303 km/s in 1902 to a high (observed) value of 545 km/s in 2003. Table 4 gives the yearly average values of *IHV*, B and V calculated as the average of the rotations spanned by each year.

6.5. Comparison With *BV* Derived From Polar Cap Potential

[43] *Le Sager and Svalgaard* [2004] derived yearly averages of *BV* from a study of the amplitude of the diurnal variation of the geomagnetic elements recorded at the polar cap stations Thule and Godhavn. The horizontal component of the geomagnetic field measured within the polar regions has a particularly simple average diurnal variation: the end point of the component vector describes a circle with a diameter (the "range," E) of typically 100 nT. E is controlled by season (ionospheric conductance) and by the interplanetary electric field as measured by *BV* mapped down along field lines to the polar cap. Averaging over a full year eliminates the seasonal dependence on conductivity and yearly average ranges have a strong ($R^2 = 0.9$) linear relationship $BV = kE$ with *BV* calculated from B and V measured by spacecraft. This relationship holds for any station within the polar caps with only a slight variation of k. A small constant term is not statistically significant, so it is not considered further. We have determined k for three polar cap stations: Thule (data back to 1932, $k = 24.9$ for V in km/s, B and E in nT) and Godhavn (back to 1926, $k = 32.0$) in the northern polar cap and Scott Base (back to 1957, $k = 27.9$) in the southern polar cap. Figure 20 compares the product *BV* calculated from B and V derived from the *IDV* and *IHV* indices and derived from the polar cap stations. We note substantial quantitative agreement between these completely independent determinations.

6.6. Comparison With Polar Cap Potential From 1902 to 1905

[44] The noted Norwegian explorer Roald Amundsen wintered over with his ship "Gjøa" at "Gjøahavn" in northern Canada close to the magnetic pole. Magnetic recordings began on 1 November 1903 and continued through May 1905 [*Steen et al.*, 1933]. The National (British) Antarctic Expedition of 1901–1904 under Robert F. Scott operated magnetographs at the Winter Quarters (sometimes known as Discovery Bay or Hut) of the Expe-

dition for nearly 2 full years (1902–1903) [*Chree*, 1912]. The range of the diurnal variation has been determined for these two sets of observations and is shown in Figure 21. Magnetographs were in operation at Cape Evans, the base station of the British (Terra Nova) Antarctic Expedition during 1911 and 1912. Cape Evans and Winter Quarters are colocated with Scott Base. The range was also determined for this station. However, this value represents only a lower limit to the true range because disturbed days, where the trace was not complete, were excluded. These early determinations are also shown in Figure 20 using k values derived from the modern data (using the k value for Godhavn (Qeqertsuaq) for Gjøahavn, as these two stations have nearly the same corrected geomagnetic latitude).

[45] In order to compare with modern values, we select years (for SBA) where the sunspot number R_z was similar (namely, 14) to R_z in 1903, namely 1965, 1975, 1976, 1985, 1986, 1995, and 1996. For GDH we select years where R_z was similar (42) to R_z in 1904 (and on the ascending branch only), namely 1966, 1977, 1987, 1997, and 1998. Then we derive *BV* for the modern years using observed B and V as shown in Table 5.

[46] The range of the polar cap variation is measured using the Y component (in a local coordinate system where the X axis coincides with the average direction of the H component). Going back to ~1900, the main field increases 6.5% at SBA/HUT and 9% at GDH/GJO. If we decrease the ionospheric conductivity by the same amounts, we decrease ΔY proportionally to $\Delta Y'$ as shown. Assuming *BV* scales with $\Delta Y'$, we get for HUT: $BV = 78.4/84.4*2493 = 2316$, and for GJO: $BV = 71.1/75.0*2560 = 2427$. If V in 1903 were the same as for the modern group of years (446 km/s) for SBA, we obtain $B = 2316/446 = 5.19$ nT. If V in 1904 were the same as for the modern years (414 km/s) for GDH, we obtain $B = 2427/414 = 5.86$ nT. These values compare favorably with B derived from the *IDV* index. If the solar wind speed a hundred years ago were somewhat lower (as we deduce in this paper), B would be correspondingly, if only slightly, higher. We take this as evidence for B ~100 years ago not being lower than now by any significant amount.

7. A Plea for Assistance With Early Data

[47] Table 6 shows an incomplete compilation of early observatories that have data suitable for calculation of *IHV*. Because almost none of the pre-1920 data is available from the World Data Centers, the authors ask the geomagnetic community for help in collecting and preserving the large body of early data, if you have any access to or knowledge of the whereabouts of data from stations listed in the table. There is a vast amount of 19th and early 20th century data in existence. An effort should be made to move all available data into electronic form for general use by all. Some examples: *Nevanlinna* [2004] reports a modern reduction of 10-min observations from Helsinki 1844–1857 and with coarser resolution until 1912. *Moos* [1910] describes the superb Colaba observations going back to 1846. *Chapman*'s [1957] analysis of the solar daily variation was based on "more than a million hourly values of the magnetic elements [from Greenwich]. This great series of observations was begun in 1838 by Airy." *IHV* indices could possibly be

constructed from nighttime subsets of these and other observations, once the data is put in digital form. There are early 19th century data from Paris, Prague, Milan, Munich, and other places. It is quite possible that some of that data may be usable for derivation of approximate *IHV* indices.

8. Conclusion

[48] In the present paper we have provided a detailed derivation of the *IHV* index and used it, in conjunction with the newly developed *IDV* index [*Svalgaard and Cliver*, 2005], for a reconstruction of solar wind speed from 1890 to present. In addition, comparison of the *IHV* index with the widely used *aa* index reveals calibration errors in *aa* prior to 1957 as suggested by *Svalgaard et al.* [2003, 2004] and substantiated by others [*Jarvis*, 2005; *Mursula and Martini*, 2006; Lockwood et al., submitted manuscript, 2007]. The *IHV* index will need to incorporate additional early data, both to corroborate data from ~1880 to 1920 and to extend the index back in time. Such work in is progress with preliminary results already back to 1844.

Appendix A

A1.   Nonremoval of "Residual" Regular Variation

[49] *Mursula et al.* [2004] suggest that it is necessary to identify and remove any possible "residual" S_R variation before calculating *IHV*. The main argument for this is that the diurnal variation of some of the geomagnetic elements does not show the characteristic flat "plateau" at high-latitude stations such as SIT and SOD during the night hours (themselves somewhat ill-defined at high latitudes). At such high latitudes the signatures of the eastward and westward auroral electrojets are clearly seen before and after midnight, respectively. We would ordinarily consider those signatures as part of "geomagnetic activity" and so see no need to remove them (apart from not knowing how to do this in any nonobjectionable way). The proper thing to do is simply not to treat *IHV* computed for high-latitude stations as comparable to *IHV* calculated from middle- and low-latitude stations. Figure A1 shows the local time diurnal variation of the unsigned difference between the values of the horizontal component for 1 hour and the next for bands of corrected geomagnetic latitude intervals from the equator to the pole. Note the effect of ring current decay through the day at middle- and low-latitude stations. It is clear that stations above ~55° have a different activity "profile" than stations below that latitude.

A2.   Use of Hourly Values Instead of Hourly Means in Older Data

[50] Originally (i.e., more than ~150 years ago), magnetic measurements were eye-readings taken at discrete times. Magnetic data yearbooks (often containing meteorological data as well) giving data for each hour (usually on the local hour mark) were published as a reasonably compact representation of the variation of the various elements. After continuous recording was introduced by *Brooke* [1847], the sheer mass of data soon overwhelmed the observers and the yearbooks still contained only hourly values. *Schmidt* [1905] pointed out that hourly means would

use the records more fully than just the instantaneous hourly values and would also "eliminate the accidental character of chance disturbances". Starting with the 1905 yearbook, Schmidt published hourly means for Potsdam (POT) (modern replacement station is now Niemegk (NGK)) near Berlin and soon most observers followed his lead, although for some it took quite some time (Chambon-la-Forêt (CLF) changed from hourly values to hourly means only in 1972). Owing to the higher variability of instantaneous values as compared to the smoother mean values, *IHV* is considerably higher (up to 50% for some stations) when computed from instantaneous values rather than from mean values. Using modern 1-min values, we can readily create a data set with near instantaneous values spaced 1 hour apart as well as calculate hourly means from 60 one-minute values. At our urging, *Mursula and Martini* [2006] came to the same conclusion. Figure A2 shows *IHV* for NGK calculated from the hourly values (denoted IHV_{01}) and from the hourly means (denoted IHV_{60}).

[51] As Figure A2 shows, in a first approximation, we have to multiply IHV_{01} by 0.7065 to reduce the values to IHV_{60}. The importance of this reduction was not clear in our preliminary study of *IHV* [*Svalgaard et al.*, 2004]. For times when geomagnetic activity is low, the difference between hourly values and hourly means becomes smaller and IHV_{01} approaches IHV_{60}. Applying a constant, average conversion factor between IHV_{01} and IHV_{60} will thus tend to slightly underestimate the IHV_{60} calculated from IHV_{01}. This has the undesirable side effect of introducing a slight, and spurious, solar cycle dependence for the ratio between IHV_{60} and IHV_{01}. A better fit is a power law applied to the daily values of *IHV*. Table A1 gives the parameters a and b for power laws $y = ax^b$ and times of changeover from hourly values to hourly means that we have determined for the stations used. Some of these times are dictated by the timing of data gaps rather than positive knowledge of when the changeover actually took place. If no 1-min data were available, the approximate method used for Figure A2 is used.

A3.   Dealing With Extreme Activity

[52] Indices like *am* and *aa* that are derived from *K* indices are capped at the top amplitude associated with $K = 9$. At times of great disturbance, *IHV* can be very large, exceeding even this maximum amplitude. An example of this is evident even in the monthly means in Figure 2. We wish to limit (or cap) *IHV* at a suitable maximum amplitude to avoid such extremes. Experiments show that a cap of 7 times the average *IHV* largely eliminates such chance outliers. If the difference is larger, it is set equal to the cap value. This happens about 0.25% of the time. Figure A3 shows rotation averages of *Am* (black curve) compared to *IHV* from NGK (blue curve) (scaled to *Am* using equation (4)) derived using the cap. The red curve (it is there but almost always hidden behind the blue curve) shows what *IHV* would have been without the cap. It is clear that the cap is needed to make the blue curve match the black curve and to prevent the red "spikes."

A4.   Station Specific Artifacts in Archival Data
A4.1.   Curious Case of Eskdalemuir

[53] The 100 years of records from ESK could be an important source of *IHV* in the European-African longitude

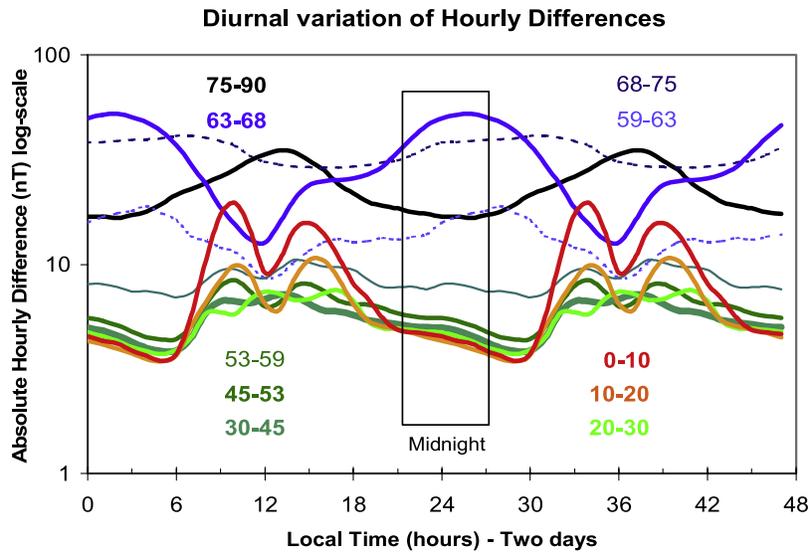**Diurnal variation of Hourly Differences**

Figure A1. Diurnal variation of unsigned hourly differences (between one hour and the next) for the H-component as a function of local time shown for corrected geomagnetic latitude bands for all available stations during 1996–2003 (color-coded from red at the equator through green at midlatitudes to blue and black in the polar regions). A band contains all stations from both hemispheres described in section 3.3. The time extends over 2 days to position the 6-hour midnight interval used for *IHV* in the middle of the figure.
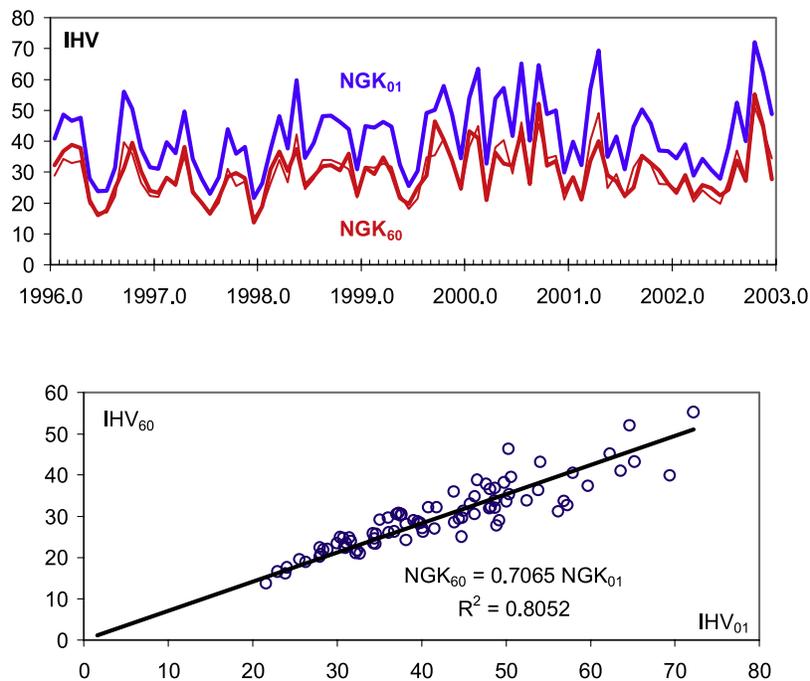

Figure A2. (top) Monthly means of *IHV* for Niemegk (NGK) 1996–2002. The heavy red curve shows *IHV* calculated from true hourly means (calculated as the mean of 60 one-minute values of the H component). The blue curve shows *IHV* calculated from a single 1-min value taken each hour on the hour. The thin red curve shows the blue curve scaled down by the coefficient determined by the linear regression shown in the lower panel. (bottom) Correlation between the monthly means of *IHV* shown in the upper panel calculated from hourly means (IHV_{60}) versus calculated from hourly values (1-min averages taken once an hour, IHV_{01}).

Table A1. Parameters *a* and *b* for the Power-Law Conversions (*Hourly Mean Value*) = *a* (*Hourly Instantaneous Value*) *b* Where the Conversion Should Be Done to Data Before the Year Indicated

Obs.	*a*	*b*	Before	Note
POT	1.1715	0.8668	1905	Assumed the same as for NGK
WLH	1.1715	0.8668	1912	Assumed the same as for NGK
CLH	1.1859	0.8756	1915	Assumed the same as for FRD
VQS	1.0415	0.9286	1915	Assumed the same as for SJG
TUC	1.1008	0.9049	1915	
HON	1.2595	0.8701	1915	
API	1.7190	0.6856	1929	Noisy
KAK	1.0890	0.9316	1955	
TOK	1.0890	0.9316	1913	Assumed the same as for KAK
DBN	0.7000	1.0000	1938	Linear fit to SED
WIT	0.7890	1.0000	1984	Linear fit to NGK
ESK	0.7119	1.0000	1919	Multiply by 1.484 before 1932 (see text)
VLJ	1.0312	0.9096	1938	Assumed the same as for CLF
CLF	1.0312	0.9096	1972	
VSS	0.8666	1.0000	1926	Multiply by 1.45 in 1921/8–1925/3 (see text)
PIL	0.8450	1.0000	1949	Comparison with SJG
SVD	0.7235	1.0000	1932	Linear fit to ABG

sector. Both *Mursula et al.* [2004] and *Clilverd et al.* [2005] analyzed *IHV* derived from ESK and found very small values in the early one third of the 20th century supporting their notion of a significant centennial change of geomagnetic activity since then. Examination of the original yearbooks from ESK (one of us (LS) visited the observatory on the occasion of its centenary) revealed that the data available from the WDCs has been processed to simulate hourly means centered on the half hour. Up through 1917, ESK reported instantaneous values on the whole hour; thereafter, until 1932, ESK reported hourly means but still centered on the whole hour. Figure A4 shows data from the WDC plotted together with data from the original yearbook for 30 January 1924. It is unmistakable that the WDC data is simply interpolated between the whole-hourly data given in the yearbook. Such smoothing greatly diminishes the variability of the data to the point where *IHV* becomes ~35% too small. Creating a synthetic interpolated dataset from modern data shows that to "undo" the effect of the smoothing, it is necessary (and it suffices) to multiply the *IHV* calculated from the smoothed data by 1.485. This removes the ESK anomaly and brings ESK into agreement with other stations [*Martini and Mursula*, 2006] but, of course, also invalidates conclusions based on the uncorrected ESK data [e.g., *Mursula et al.*, 2004; *Clilverd et al.*, 2005].

A4.2. Quality Control of WDC Data

[54] A large database invariably contains errors of many types: timing, calibration, sign, transcription, omission, and misunderstanding. Information about the data (metadata) is sorely lacking, especially for older data in the classical WDC data format. Fortunately, the data themselves can often be analyzed to bring to light many errors and allow correction of much of the data. Unfortunately, it is difficult to propagate such corrections back into the publicly available databases. This section details our experience with a typical case, Vassouras (VSS) near Rio de Janeiro. The observatory has been in continuous operation since 1915 and is important as the longest-running station in its longitude sector in the Southern Hemisphere. Figure A5 shows the diurnal variation of the horizontal component through the years. It is evident that about half of the data is not in the WDCs. The daily maximum occurs at 14.7 hours UT or 11.8 hours local time. The data from the WDC is consistent with this but only during 1957–1959 and 1998–present. At other times the maximum occurs 3 hours earlier (after about 1925) or 3.5 hours earlier (before that). The early WDC data thus seem to be hourly instantaneous values taken at the whole hour and then hourly means centered at the half hour (some time after 1925) according to local standard time (Brazil started to use standard time 1 January 1914) rather than UT. We shifted the hourly data
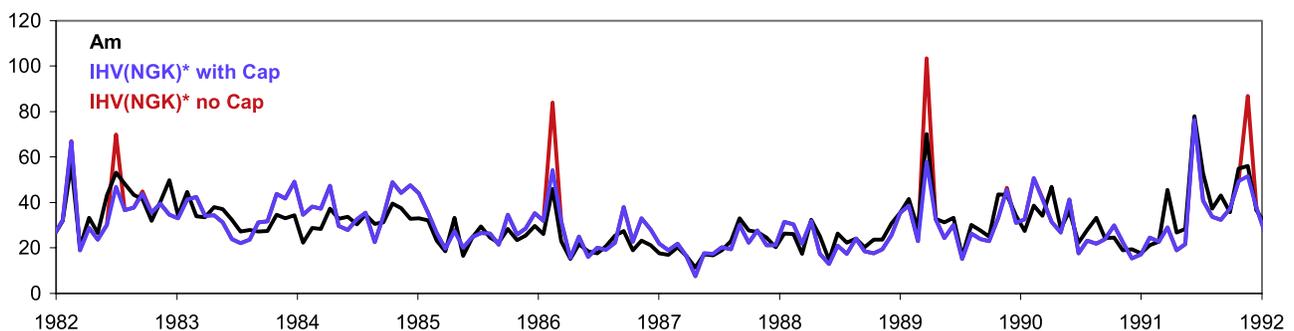

Figure A3. Rotation averages of *Am* (black curve) compared to *IHV* from NGK (blue curve) (scaled to *Am* using equation (4)) derived using the cap. The red curve (almost always hidden behind the blue curve) shows what *IHV* would have been without the cap.
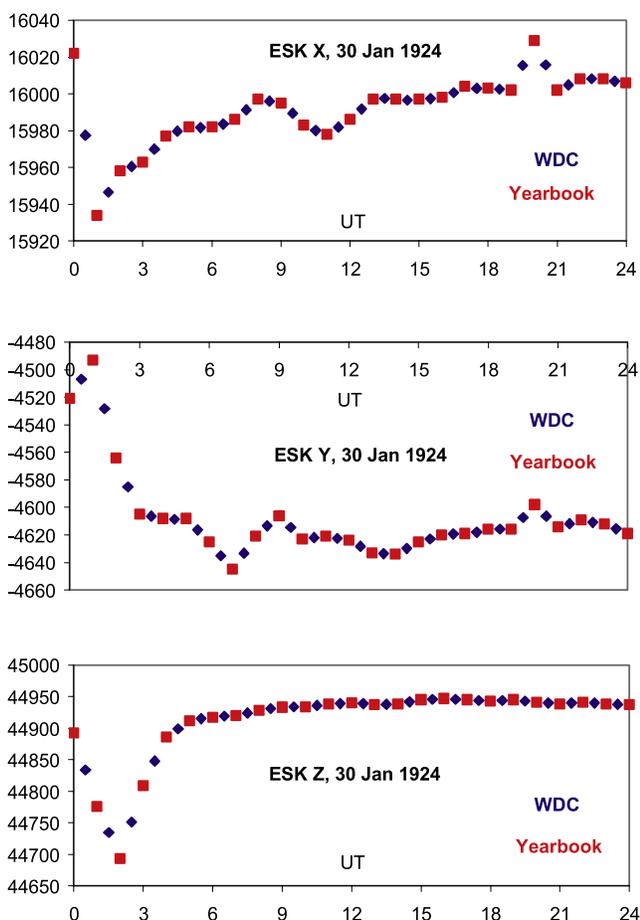
Figure A4. The variation of geomagnetic components X, Y, and Z on 30 January 1924 for ESK plotted using the hourly values supplied by the WDCs (blue diamonds) and given in the original observatory yearbook (red squares). It is unmistakable that the WDC data is simply interpolated between the whole hourly data given in the yearbook.

points to 4 hours later before 1926 and to 3 hours later for 1949–1997 except for the IGY data 1957–1959 that has already been shifted in the WDC data. It is unknown (to us) when the change from hourly values to hourly means took place, although the time of the Second Polar Year 1932–1933 would be a likely candidate.

[55] The tables in the yearbooks that give the hourly data values are conventionally based in the sense that actual value of the field is Field = Base ± Tabular Entry. The sign of the tabular entry is usually a plus sign, but occasionally a minus sign is used, e.g., as evidenced in an indirect way by this quote from a Batavia (BTV) yearbook "increasing numbers denote decreasing easterly declination." Such subtlety is often lost during the data entry process (partly because the sign used may change without warning for a given station at any time). The base sometimes changes during a year as well. This also is often not caught at data entry so that the data values entered are off by (usually) a multiple of 100 (e.g., H component for the year 1957 and August 1959 for VSS, except the first 3 hours because of the local time to UT shift). Base and sign changes may be difficult to correct because the data may have been reformatted later (maybe even at the WDC). This seems to have happened to the VSS

data because the diurnal maximum at 11.8 hours local time occurs as a minimum during the interval January 1915 through May 1918, yet the base value is the same on either side of 31 May 1918. We changed the sign of the tabular entries and adjusted the base values before June 1918, removed spurious data, e.g., for 31 November 1972 (in data from WDC Kyoto), corrected base offsets when they were clearly wrong, and decided to completely omit data for April 1991 because the tabular entries were in units of 10 nT rather than 1 nT (inferred from a tenfold diminution of the variability during that month), and still there were errors left as detailed in the discussion of VSS in section B.6. The main point here is to emphasize that the data in the WDCs contain errors that realistically can only be reliably corrected at or with cooperation from the observing stations themselves as the necessary metadata may only be available locally at the observatories or their managing institutions.

[56] A few other examples further illustrate problems of data quality. The data for VQS is given in local time rather than UT, and the data for the series POT-SED-NGK has the 7th through the 10th day of every January for many early years designated as "missing," although the data is present in the yearbooks and in older versions of the electronic data. Apparently, some recent "cleanup" was attempted with unintended consequences. For years from 1900 through 1907, the WDCs at times have "Y2K" problems where there is confusion about 2000–2007 and 1900–1907, as the century has no unique designation within the "WDC Exchange Format." Attempts by the WDCs to rectify these various problems have often led to introduction of other problems or to loss of data, and there is no standard procedure for feedback from researchers to the WDCs.

A5. Secular Changes of the Earth's Main Field
A5.1. Influence of Changing Corrected Geomagnetic Latitude

[57] As Figure 6 shows, *IHV* for stations close to or polewards of 55° is very sensitive to changes in the stations' corrected geomagnetic latitude. *Mursula et al.* [2004] analyzed *IHV* derived from (among others) SOD ($\sim$63°) and *Clilverd et al.* [2005] analyzed *IHV* derived from (among others) LER ($\sim$59°). Both these stations are polewards of 55° and should not be directly compared with results from lower latitudes. Figure A6 shows why. From 1900 to 2005, the corrected geomagnetic latitude of LER decreased from 59.35° to 57.98°, while SOD increased from 62.35° to 64.10°. Using equation (3), we calculate *IHV* for these stations for every 5 years and plot the percentage change relative to their mean values over the time interval. The total change is +27.5% for SOD and −36.5% for LER. Owing to their lower latitude, the change for ESK is smaller (−6.5%) and for NGK is negligible (+0.5%) (part of the reason that NGK was chosen as reference station).

[58] It is instructive to calculate *IHV* from the actual data for LER and SOD (the latter scaled by 0.2579 to match the mean of LER). Corrected geomagnetic latitude is determined using the International Geomagnetic Reference Field IGRF/DGRF models supported by the http://modelweb.gsfc.nasa.gov/models/cgm/cgm.html Web site. The lower panel in Figure A6 shows the ratio LER/(scaled SOD) for each Bartels rotation since 1926. The red line shows the ratio expected, using equation (3), due to the changing latitudes: a steady
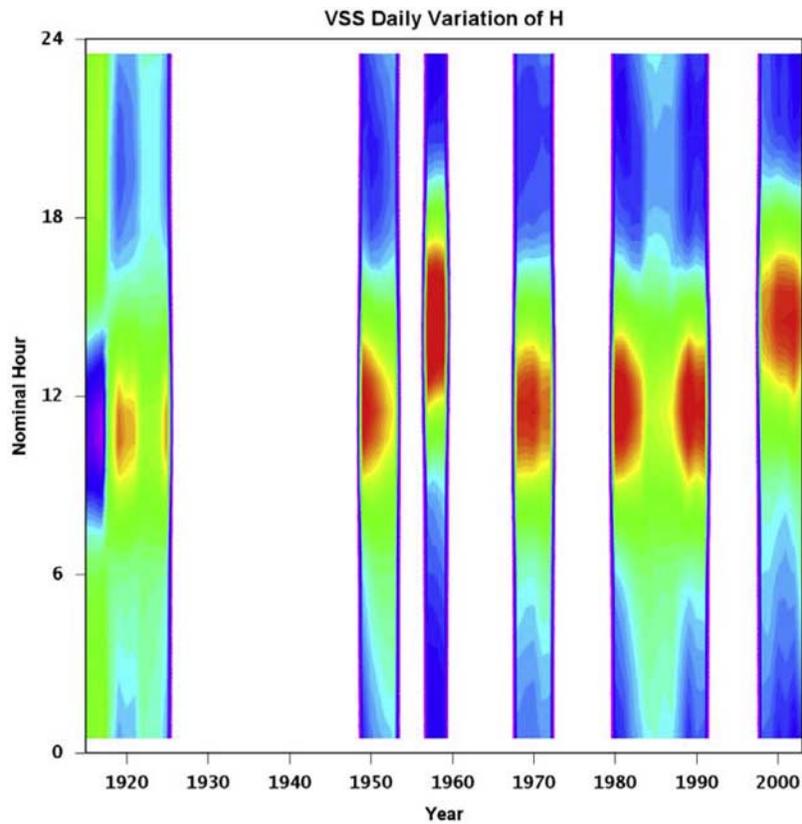
Figure A5. The diurnal variation of the horizontal component through the years for Vassouras (VSS) near Rio de Janeiro. The observatory has been in continuous operation since 1915 and is important as the longest running station in its longitude sector in the Southern Hemisphere. The plot is a contour plot of the variation of the H component about its daily mean as a function of the hour as given in the WDC data (the "nominal" hour). Colors from purple/blue to orange/red signify the range from low (negative) to high (positive) values. White areas show where data is missing from the WDC archive.
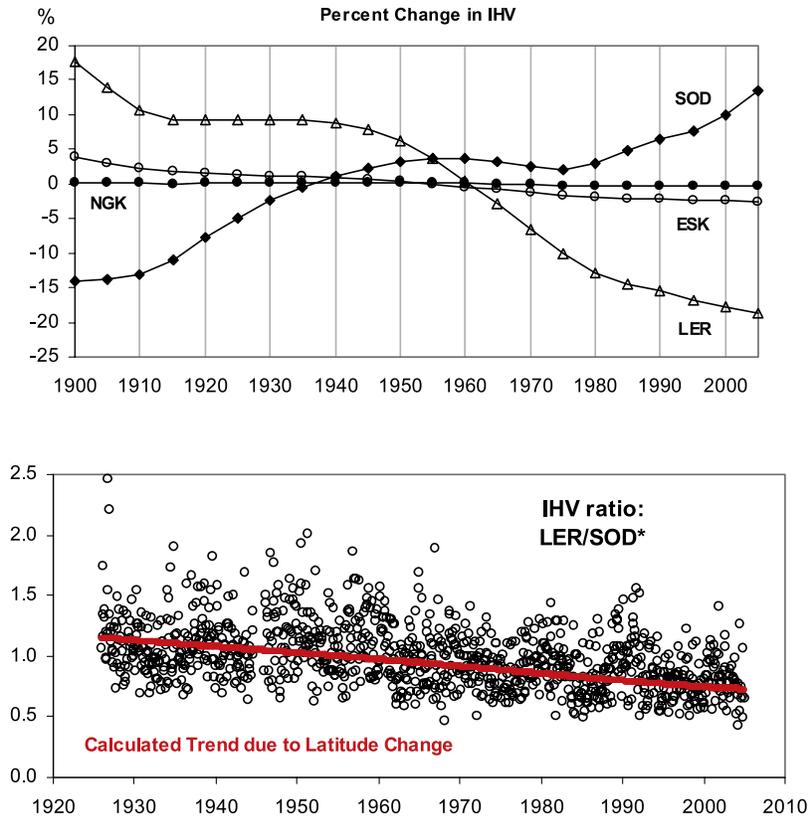
Figure A6. (top) Percentage change relative to the mean values over 1900–2005 of *IHV* expected for LER, SOD, ESK, and NGK (using equation (3)) resulting from actual changes in corrected geomagnetic latitude for these stations. (bottom) The ratio LER/(scaled SOD) for each Bartels rotation since 1926 of calculated *IHV* from the actual data for LER and SOD (the latter scaled by 0.2579 to match the mean of LER). The red line shows the ratio expected (from equation (3)) due solely to the changing latitudes.
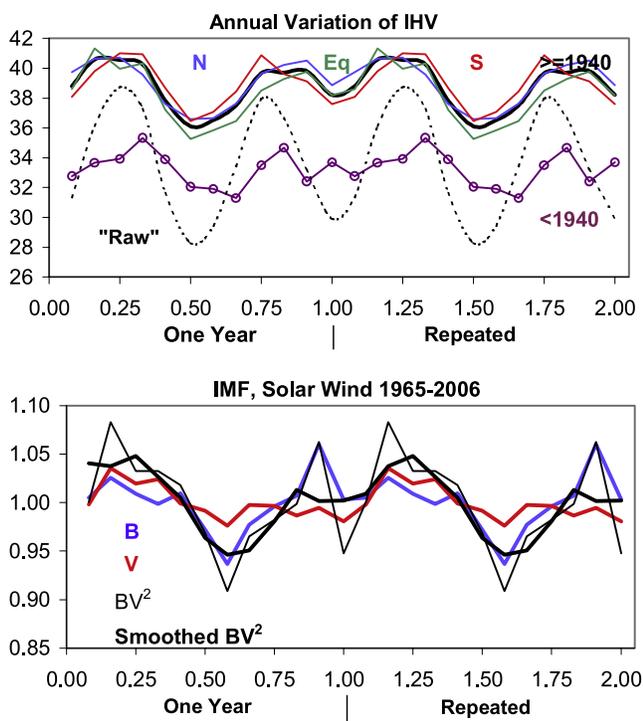
Figure A7. (top) Annual variation of *IHV* for the composite Northern Hemisphere (blue), Southern Hemisphere (red), and equatorial (green) series for years 1940 to the present. The average of these three series is shown with a thick black curve. Below this curve we show (purple curve with open circles) the average annual variation of the full *IHV* series for years before 1940 where the data is sparser, especially for the Southern Hemisphere. The dotted curve shows the variation of the "raw" *IHV* (i.e., not corrected for the dipole tilt). To better show the annual variation, we have repeated the curves for yet another year in the right-hand portion of the figure. (bottom) Average annual variation of IMF *B* (blue), solar wind speed *V* (red), and the product BV^2 (thin black) relative to their mean values for 1965–2006. The heavy black curve shows a three-point running mean of normalized BV^2. It would seem that most of the annual variation of *IHV* can be explained simply as variation of the driving BV^2.

decrease totaling 46%. We note good agreement and also that the effect is large. These stations should not be used without correcting for the secular change of latitude, or better, not used at all as representative for any purported global change on account of their latitude being too high. This invalidates the conclusions of *Mursula et al.* [2004] and *Clilverd et al.* [2005] regarding long-term changes of the solar wind. For all stations ultimately used (as indicated in Table 1) we have verified that the changes of *IHV* due to secular changing corrected geomagnetic latitudes are small and of varying sign such as to be negligible in a composite time series.

A5.2. Influence of Decreasing Main Field

[59] The dipole moment of the Earth's main magnetic field has decreased significantly over the past centuries, influencing both the size of the magnetosphere and the conductivity of the ionosphere. *Glassmeier et al.* [2004] found that ring current perturbations (measured by the *IDV*

index) do not increase with decreasing dipole moment *M* and suggest that the magnetic effect, *b*, of the polar electrojets (partly measured by the *IHV* index) scales very weakly with *M*, namely, as $M^{1/6}$. If so, the 9% decrease of *M* since 1850 would only result in a 1.5 % decrease of *b* which would be too small to reliably detect. On the other hand, there is evidence [*Svalgaard and Cliver*, 2007] that the conductance of the midlatitude ionosphere has increased by 10% since 1840. This increase is reflected in the amplitude of the S_R variation, but it is not clear what effect that has on nighttime geomagnetic activity. We therefore do not attempt to correct for the change in the main field. It is, however, an important and as yet unresolved question what the effect of a changing main field has on observed geomagnetic activity. In the present paper we assume that to first order the effect can be ignored. This assumption may not be valid, so all results are appropriately qualified.

A6. Missing Data During Storms

[60] There are some effects that can lead to an underestimation of *IHV*, such as data missing because of the magnet moving too rapidly or the recording going off scale. A typical example is the very brief magnetic storm of 25 September 1909, possibly the strongest storm during the entire interval 1882–2006 (J. J. Love, personal communication, 2006). We suggest using other indices like the *aa* index to infer *IHV* for times with missing data as follows. For the interval of 27 Bartels rotations (∼2 years) centered on the rotation containing the storm sudden commencement, a "sectorial" *aa* index can be computed for each rotation as the average for that rotation of the *aa* index over the UT intervals matching as closely as possible the 6-hour intervals used for the calculation of *IHV* for the six longitude sectors. Omitting the data for the rotation with the storm (or missing data in general), the *aa* values are then scaled (see Appendix B) to the average of *IHV* for each sector. Applying the scale factors so gained, *aa* can now be scaled up to estimate *IHV* for the corresponding sectors (both north and south) during the rotation with the storm-related missing data. Because each storm is handled separately, correct calibration and long-term stability of the *aa* or other indices are not essential. The estimate is crude but is better than having no estimate at all. For times where no other indices are available one could use a "climatological" storm profile. We have not yet carried out this procedure for the present investigation.

A7. Lack of Consistent Summer/Winter Difference

[61] Even though we have removed the dominant equinoctial contribution of the semiannual variation, we expect a residual semiannual variation due to axial and Russell-McPherron effects, as well as a possible difference related to the seasons (summer/winter). Figure A7 shows the variation of *IHV* with month of year. The upper panel shows the annual variation of *IHV* for the Northern Hemisphere (blue), Southern Hemisphere (red), and composite equatorial (green) series for years 1940 to the present. The average of these three series is shown with a thick black curve. Below this curve we show (purple) the average annual variation of the full *IHV* series for years before 1940 where the data is sparser, especially for the Southern Hemisphere. In spite of the larger noise level, the same

general variation is found in this subset as well, namely a superposition of an annual wave with extrema near aphelion and perihelion and a semiannual variation with extrema near the usual times.

[62] The dotted curve shows the variation of the "raw" *IHV* (i.e., not corrected for the dipole tilt modulation). To better show the annual variation, we have repeated the curves for yet another year in the right-hand portion of Figure A7. The residual variation (after correction) is about 25%, consistent with several studies [e.g., *Svalgaard et al.*, 2002, and references therein]. Drawing on a result of section 6, we expect the residuals to be largely driven by BV^2. This seems to be the case as shown by the bottom of Figure A7 that depicts the average annual variation of IMF B (blue), solar wind speed V (red), and the product BV^2 (thin black) relative to their mean values for 1965–2006. The heavy black curve shows a three-point running mean of the normalized BV^2. Well aware of the danger of overinterpreting noisy data, we suggest that the dominant variation of B is an annual wave with minimum near aphelion and maximum near perihelion. The amplitude of this annual wave is consistent with what we would expect from the variation of the distance from the Sun due to the eccentricity of the Earth's orbit. With this interpretation, most of the annual variation of *IHV* is explained and there seems to be little room for an intrinsic systematic local summer/winter difference.

Appendix B

B1. European-African Sector (15°E)

[63] We start in the north. NGK replaced SED in 1932, so the first task is to bridge SED and NGK. The four stations VLJ, ABN, RSV, and DBN overlap the transition from SED to NGK. Table B1 gives the scale factors to apply to *IHV* derived from the station in the first column to SED and NGK, respectively. The ratio between these factors is the scale factor for normalizing SED to NGK; we adopt for this value the average (0.9349 ± 0.0082) of the four stations.

[64] The next step is to multiply SED by its scaling factor to NGK and join the scaled SED to the NGK series for a combined SED-NGK series. Then we regress the four stations against this combined series and arrive at the final set of scale factors shown in Table B2.

[65] Although RSV (Rude Skov) continued operation through 1981, the data after 1978 is too noisy to be of any use. Extension of a nearby electric trainline necessitated relocating the observatory to rural Brorfelde. RSV goes back to 1908 and VLJ to 1901. Their predecessor stations, COP and PSM, operated from 1891 and 1883, respectively, and data exist, but not yet in electronic form.

[66] There are three further dates of concern: the interruption of observations at the end of World War II, the start of the IGY (when some observatories improved instruments and/or reduction procedure), and the introduction of digital recording in the 1980s. To verify the stability of NGK from 1932 to the present, we compare with FUR, WNG, WIT, BFE, HAD, and CLF. Table B3 gives the scale factors to NGK for these stations.

[67] There are no indications of any problems or systematic differences and the correlations are uniformly high, so we conclude that the calibration is stable and that all these stations support each other. Note that we did not include ESK in this group because of its proximity to the auroral zone and the problems with its WDC data set described in section A.4.1.

[68] There remains to join POT to the reference series. DBN data from 1903 through 1938 form the bridge between POT and NGK. The scale factors are given in Table B4 from which we derive the scale factor from POT to NGK equal to (DBN → NGK/DBN → POT) = 0.9604/0.9819 = 0.9871. Hourly values from WLH (kindly supplied by J. Linthe, personal communication, 2005) overlap with POT for 1890–1895. From the overlap between WLH and POT we compute the scale factor from WLH to NGK as (WLH → POT*POT → NGK) = 0.9451*0.9871 = 0.9329.

[69] It would be highly desirable to verify and solidify these calibrations using the several other European stations observing at the time, but to date no other data exist in electronic form. We can now construct a composite series for the Northern Hemisphere European Sector (IHV15N). The average standard deviation around the mean value is 1.4 nT (*IHV* has units of nT) or 3.8%.

[70] Now, we move to the south. Suitable stations are HBK and CTO and its replacement station HER. Their scale factors to NGK are given in Table B5. Whether or not there is a real intrinsic difference in geomagnetic activity between the two hemispheres is not known and we shall leave it at that, normalizing to NGK. Finally, IHV15S is scaled to IHV15N. The scale factor is given in Table 3.

B2. Siberian-Indian Sector (75°E)

[71] We start in the north. We select ABG (digital data for 1924–2004) as reference station for this sector, then compute the average of all stations in the sector (becomes IHV75N), and finally scale that average to IHV15N. As with the question of intrinsic north/south difference we also force all sectors to (ultimately) the same level as NGK. We have already compensated for the (real) UT difference between sectors (see section 3.2). Table B6 gives the scale factors to ABG. Finally, IHV75N is scaled to IHV15N. The scale factor for IHV75N to IHV15N is given in Table 3.

[72] Now, we move to the south. Suitable stations are AMS, CZT, and PAF, although PAF is at an uncomfortably high corrected geomagnetic latitude (−58°) and its scaling to AMS is therefore decidedly nonlinear (IHV_{AMS} = 2.114 $IHV_{PAF}^{0.634}$; R^2 = 0.85). We then construct IHV75S as the mean of AMS and the scaled CZT and PAF. Table B7 gives the scale factor for CZT to AMS. Finally, IHV75S is scaled to IHV15N. The scale factor is given in Table 3.

B3. Japanese-Australian Sector (130°E)

[73] We start in the north. We select KAK as reference station for this sector, deduce the scaling factors for the other stations in this sector, then compute the average of the scaled values (becomes IHV130N), and finally scale that average to IHV15N. Suitable stations are MMB, KNY, and SSH. Table B8 gives the scale factors to KAK for these stations. Data for Tokyo (TOK) was kindly supplied by T. Koide (personal communication, 2005). TOK was "bridged" to KAK using IHV15N. Undigitized data for this sector exist to eventually improve this bridge. The scale factor for the composite IHV130N to IHV15N is given in Table 3.

[74] Now, we move to the south. The Australian stations all fall in this sector. We select GNA as reference station (1957–

Table B1. Scale Factors to Be Applied to IHV Derived From Stations in the 15°N Sector to Normalize the Data for the Station Mentioned in the "From" Columns to SED and NGK As Shown[a]

From	SED	R^2	Time	NGK	R^2	Time	NGK/SED
VLJ	1.2045	0.87	1923–1931	1.1399	0.77	1932–1936	0.9463
ABN	1.1196	0.94	1926–1931	1.0370	0.88	1932–1956	0.9263
RSV	1.0077	0.96	1927–1931	0.9233	0.89	1932–1978	0.9163
DBN	1.0103	0.85	1908–1931	0.9604	0.80	1932–1938	0.9506
							0.9349

[a]The last column gives the ratio of the factors to NGK and to SED. See text for details.

Table B2. Scale Factors to Be Applied to IHV Derived From More Stations in the 15°N Sector to Normalize the Data for the Station Mentioned in the "From" Column to NGK for the Time Intervals Indicated

From	NGK	R^2	Time
VLJ	1.1399	0.85	1923–1936
ABN	1.0364	0.89	1926–1956
RSV	0.9233	0.90	1927–1978
DBN	0.9604	0.84	1908–1938
SED	0.9349	Adopt	1908–1931

Table B3. Scale Factors to Be Applied to IHV Derived From More Stations in the 15°N Sector to Normalize the Data for the Station Mentioned in the "From" Column to NGK for the Time Intervals Indicated

From	NGK	R^2	Time
FUR	1.1251	0.96	1940–2004
WNG	0.9269	0.97	1943–2004
WIT	1.0037	0.97	1939–1984
BFE	0.9403	0.95	1981–2004
CLF	1.1466	0.87	1936–2004
HAD	1.0823	0.89	1957–2004

Table B4. Scale Factors to Be Applied to IHV Derived From Stations in the 15°N Sector to Normalize the Data for the Station Mentioned in the "From" Columns to POT and NGK As Shown

From	POT	R^2	Time	NGK	R^2	Time
DBN	0.9819	0.90	1903–1907	0.9604	0.80	1932–1938
POT				0.9871	Adopt	1890–1907
WLH	0.9451	0.81	1883–1895	0.9329	Adopt	1883–1895

Table B5. Scale Factors to Be Applied to IHV Derived From Stations in the 15°S Sector to Normalize the Data for the Station Mentioned in the "From" Column to NGK for the Time Intervals Indicated

From	NGK	R^2	Time
CTO	1.4342	0.76	1932–1940
HER	1.3505	0.80	1941–2004
HBK	1.2215	0.73	1973–2004

Table B6. Scale Factors to Be Applied to IHV Derived From Stations in the 75°N Sector to Normalize the Data for the Station Mentioned in the "From" Column to ABG for the Time Intervals Indicated

From	ABG	R^2	Time
SVD	1.1251	0.78	1930–1980
TFS	0.8190	0.81	1957–2001
TKT	0.9847	0.90	1957–1991
NVS	0.8592	0.82	1967–2003
AAA	0.9340	0.86	1963–2002
ARS	0.9009	0.79	1973–2002

Table B7. Scale Factors to Be Applied to IHV Derived From Stations in the 75°S Sector to Normalize the Data for the Station Mentioned in the "From" Column to AMS for the Time Intervals Indicated

From	AMS	R^2	Time
CZT	0.8420	0.83	1974–2004

Table B8. Scale Factors to Be Applied to IHV Derived From Stations in the 130°N Sector to Normalize the Data for the Station Mentioned in the "From" Column to KAK for the Time Intervals Indicated

From	KAK	R^2	Time
MMB	0.8448	0.98	1957–2006
KNY	0.9526	0.96	1958–2006
SSH	0.8148	0.92	1933–2002
TOK	0.6950	0.50	1897–1912

Table B9. Scale Factors to Be Applied to IHV Derived From Stations in the 130°S Sector to Normalize the Data for the Station Mentioned in the "From" Columns to WAT and GNA As Shown[a]

From	WAT	R^2	Time	GNA	R^2	Time	GNA/WAT
TOO	0.8549	0.84	1924–1958	0.8041	0.83	1957–1979	0.9406
CNB				0.8468	0.79	1981–2004	
WAT				0.9406	adopt		

[a]The last column gives the ratio of the factors to GNA and to WAT. See text for details.

Table B10. Scale Factors to Be Applied to IHV Derived From Stations in the 200°N Sector to Normalize the Data for the Station Mentioned in the "From" Column to HON for the Time Intervals Indicated

From	HON	R^2	Time
MID	1.0063	0.92	2000–2002

Table B11. Scale Factors to Be Applied to IHV Derived From Stations in the 200°S Sector to Normalize the Data for the Station Mentioned in the "From" Column to API for the Time Intervals Indicated

From	API	R^2	Time
AML	0.7839	0.79	1957–1978
EYR	0.7758	0.77	1978–2004
PPT	1.0455	0.85	1968–2004

Table B12. Scale Factors to Be Applied to IHV Derived From Stations in the 240°N Sector to Normalize the Data for the Station Mentioned in the "From" Column to TUC for the Time Intervals Indicated

From	TUC	R^2	Time
VIC	0.9234	0.82	1957–2004
BOU	1.0345	0.94	1967–2004
FRN	1.0626	0.89	1983–2004

Table B13. Scale Factors to Be Applied to IHV Derived From Stations in the 290°N Sector to Normalize the Data for the Station Mentioned in the "From" Columns to SJG, CLH, and FRD As Shown

From	SJG	R^2	Time	CLH	R^2	Time	FRD
CLH	0.7323	0.85	1926–1956				0.9306
FRD	0.7869	0.85	1956–2004				1.0000
VQS				1.4150	0.84	1903–1924	1.3168
SJG				1.3655	0.85	1926–1956	1.2708

Table B14. Scale Factors to Be Applied to IHV Derived From Stations in the 290°S Sector to Normalize the Data for the Station Mentioned in the "From" Column to VSS for the Time Intervals Indicated

From	VSS	R^2	Time
PIL	1.0238	0.58	1949–1985
TRW	0.9863	0.72	1957–2004

Table B15. Scale Factors to Be Applied to IHV Derived From Stations in the 290°S Sector to Normalize the Data for the Station Mentioned in the "From" Column to the Combined VSS-TRW Series for the Time Intervals Indicated

From	VSS-TRW	R^2	Time
AIA	0.8585	0.74	1957–2004
LQA	0.9904	0.75	1964–1981
SGE	0.7871	0.46	1975–1982
ARC	0.9921	0.75	1978–1995
PST	1.0006	0.92	1994–2004
LIV	0.8932	0.90	1996–2005

Table B16. Scale Factors to Be Applied to IHV Derived From Stations in the Equatorial (Within 9°) Zone to Normalize the Data for the Station Mentioned in the "From" Column to NGK for the Time Intervals Indicated

From	NGK	R^2	Time
BNG	1.1467	0.76	1955–2003
AAE	1.0607	0.78	1958–2004
TRD	1.3365	0.65	1957–1999
ANN	1.2659	0.65	1964–1999
GUA	1.4146	0.46	1957–2004
HUA	1.0917	0.48	1955–2004

2004). The earliest available data is from WAT (1919–1958). TOO (1924–1979) can then serve as bridge between WAT and GNA. For modern data, CNB (1981–2004) serves as a check on GNA. Scale factors are given in Table B9. The scale factor from WAT to GNA is (TOO → GNA/TOO → WAT) = 0.8041/0.8549 = 0.9406. Finally, IHV130S is scaled to IHV15N. The scale factor is given in Table 3.

B4.   Mid-Pacific Sector (200°E)

[75]   We start in the north. We select HON as reference station for this sector. There are data for a few years from MID. We include that data to compare with HON. As Table B10 show, the agreement between MID and HON is good. Finally, IHV200N is scaled to IHV15N. The scale factor is given in Table 3.

[76]   Now, we move to the south. We select API (1922–2004) as reference station and scale AML (1957–1978), EYR (1978–2004), and PPT (1968–2004) to API. The scale factors are given in Table B11. Finally, IHV200S is scaled to IHV15N. The scale factor is given in Table 3.

B5.   Pacific West Coast Sector (240°E)

[77]   We start in the north. We select TUC (1910–2004) as reference station for this sector because of its very long series of observations. BOU (1967–2004), FRN (1983–2004), and VIC (1957–2004) comprise the remaining stations of the sector. TEO would have been ideal but is very noisy (R^2 for correlation with TUC is only 0.24). Scale factors are given in Table B12. A power law for VIC is a slightly better fit: TUC = 1.6102 VIC$^{0.849}$ (R^2 = 0.85) and is used instead of the linear fit. Finally, IHV240N is scaled to IHV15N. The scale factor is given in Table 3.

[78]   Now, we move to the south. There are really no stations with available data. Easter Island (EIC) would be ideal, but only 15 days of data (in 1964) have been found, although yearbooks or data may be available for other years. IAGA Resolution 8 (1979) urged establishment of an observatory on Easter Island, and the French IPGP is planning such a station under the INTERMAGNET program. In anticipation hereof and for completeness we include EIC, becoming IHV240S. IHV240S is finally scaled to IHV15N. The scale factor is given in Table 3.

B6.   Americas Sector (290°E)

[79]   We start in the north. We select FRD (1956–2004) as reference station for this sector. We need SJG (1926–2004) to serve as a strong bridge between CLH (1901–1956) and FRD (1956–2004). CLH in turn bridges the gap between VQS (1903–1924) and SJG. The data in the WDC for VQS

was given in local standard time rather than UT and had to be shifted appropriately. Scale factors are given in Table B13. The scale from CLH to FRD is (CLH → SJG/FRD → SJG) = 0.7323/0.7869 = 0.9306. In a similar manner we derive the scale factors for all the stations to FRD shown in the last column of the table. Finally, IHV290N is scaled to IHV15N. The scale factor is given in Table 3.

[80]   Now, we move to the south. We select VSS (1915–2006) as reference station. Data for August 1921–1926 are too low compared to IHV290N and have been scaled up by a factor of 1.45. No metadata is available yet to help explain the reason for this discrepancy. PIL (1940–1985) and TRW (1957–2004) supply additional data, filling gaps in the series for VSS. Scale factors are given in Table B14.

[81]   Because both VSS and TRW have many data gaps, but one often has data while the other one does not, we construct a combined VSS-TRW data set (scaled to VSS) and use AIA (1957–2004), LQA (1964–1981), SGE (1975–1982), ARC (1978–1995), PST (1994–2004), and LIV (1996–2005) to fill in the holes. Scale factors to the combined VSS-TRW data set are given in Table B15. Finally, IHV290S is scaled to IHV15N. The scale factor is given in Table 3.

B7.   Equatorial Stations

[82]   A selection of stations close to (within 9° of latitude) the geomagnetic equator was evaluated for suitability. Scaling factors to NGK are given in Table B16. The decrease in correlation is due to differences in longitude and thus in local time as we progress around the globe (see section 4.2). The lowest panel of Figure 7 compares the 13-rotation running mean of a composite of the equatorial stations and the global composite discussed in section 4.2. We conclude that *IHV* can be reliably derived even this close to the equator. Figure S13 in the auxiliary material shows the detailed composite *IHV* for the equatorial stations. The equatorial stations were not included in deriving the global composite *IHV* because we want to compare *IHV* to the midlatitude range indices. In the future one might contemplate including the equatorial *IHV*.

References

Bartels, J. (1932), Terrestrial-magnetic activity and its relations to solar phenomena, *J. Geophys. Res.*, *37*, 1.

Bartels, J. (1940), Solar radiation and geomagnetism, *J. Geophys. Res.*, *45*, 339.

Bartels, J., N. H. Heck, and H. F. Johnson (1939), The three-hour-range index measuring geomagnetic activity, *J. Geophys. Res.*, *44*, 411.

Brooke, C. (1847), On the automatic registration of magnetometers, and other meteorological instruments, by photography, *Phil. Trans. London 1847*, 59.

Broun, J. A. (1861), On the horizontal force of the earth's magnetism, *Proc. R. Soc. Edinburgh*, *22*, 511.

Caballero-Lopez, R. A., H. Moraal, K. G. McCracken, and F. B. McDonald (2004), The heliospheric magnetic field from 850 to 2000 AD inferred from 10Be records, *J. Geophys. Res.*, *109*, A12102, doi:10.1029/2004JA010633.

Chapman, S. (1957), The lunar and solar daily variations of the horizontal geomagnetic vector at Greenwich, 1848–1913, *Abhandl. Akad. Wissenschaft. Göttingen Math. Phys. Kl.*, *3*, 3.

Chapman, S., and J. Bartels (1940), *Geomagnetism*, Clarendon, Oxford, U. K.

Chernosky, E. J. (1960), Geomagnetism, in *Handbook of Geophysics*, rev. ed., p. 10, Macmillan, New York.

Chernosky, E. J. (1966), Double sunspot-cycle variation in terrestrial magnetic activity 1884–1963, *J. Geophys. Res.*, *71*, 965.

Chernosky, E. J. (1983), A directly obtained geomagnetic activity measure, J3, in *Scientific Contributions in Commemoration of Ebro Observatory's 75th Anniversary*, *NASA SEE N85-13308 04-42*, p. 169, NASA, Washington, D. C.

Chree, C. (1912), *Studies in Terrestrial Magnetism*, 206 pp., Macmillan, London.

Clilverd, M. A., E. Clarke, T. Ulich, J. Linthe, and H. Rishbeth (2005), Reconstructing the long-term *aa* index, *J. Geophys. Res.*, *110*, A07205, doi:10.1029/2004JA010762.

Cliver, E. W., V. Boriakoff, and K. H. Bounar (1996), The 22-year cycle of geomagnetic and solar wind activity, *J. Geophys. Res.*, *101*, 27,091.

Cliver, E. W., V. Boriakoff, and K. H. Bounar (1998a), Geomagnetic activity and the solar wind during the Maunder Minimum, *Geophys. Res. Lett.*, *25*, 897.

Cliver, E. W., V. Boriakoff, and J. Feynman (1998b), Solar variability and climate change: Geomagnetic *AA* index and global surface temperature, *Geophys. Res. Lett.*, *25*, 1035.

Cliver, E. W., Y. Kamide, and A. G. Ling (2000), Mountains versus valleys: Semiannual variation of geomagnetic activity, *J. Geophys. Res.*, *105*, 2413.

Cliver, E. W., L. Svalgaard, and A. Ling (2004), Origins of the semiannual variation of geomagnetic activity in 1954 and 1996, *Ann. Geophys.*, *22*(1), 93, Sref-ID:1432-0576/ag/2004-22-93.

Crooker, N. U., and G. L. Siscoe (1986), The effect of the solar wind on the terrestrial environment, in *Physics of the Sun, Astrophys. and Sol. Terr. Relations*, vol. 3, edited by P. A. Sturrock et al., p. 193, D. Riedel, Norwell, Mass.

Echer, E., and L. Svalgaard (2004), Asymmetry in the Rosenberg-Coleman effect around solar minimum revealed by wavelet analysis of the interplanetary magnetic field polarity data (1927–2002), *Geophys. Res. Lett.*, *31*, L12808, doi:10.1029/2004GL020228.

Ellis, W. (1900), Raising figures, *Observatory*, *23*, 95.

Feynman, J., and N. U. Crooker (1978), The solar wind at the turn of the century, *Nature*, *275*, 626.

Fisk, L. A., and N. A. Schwadron (2001), The behavior of the open magnetic field of the Sun, *Astrophys. J.*, *560*(1), 425, doi:10.1086/322503.

Glassmeier, K., J. Vogt, A. Stadelmann, and S. Buchert (2004), Concerning long-term geomagnetic variations and space climatology, *Ann. Geophys.*, *22*(10), 3669, Sref-ID:1432-0576/ag/2004-22-3669.

Jarvis, M. J. (2005), Observed tidal variation in the lower thermosphere through the 20th century and the possible implication of ozone depletion, *J. Geophys. Res.*, *110*, A04303, doi:10.1029/2004JA010921.

Jonkers, A. R. T., A. Jackson, and A. Murray (2003), Four centuries of geomagnetic data from historical records, *Rev. Geophys.*, *41*(2), 1006, doi:10.1029/2002RG000115.

Jordanova, V. K., C. J. Farrugia, J. F. Fennel, and J. D. Scudder (2001), Ground disturbances of the ring current, magnetosphere, and tail currents on the day the solar wind almost disappeared, *J. Geophys. Res.*, *106*, 25,529.

Le Sager, P., and L. Svalgaard (2004), No increase of the interplanetary electric field since 1926, *J. Geophys. Res.*, *109*, A07106, doi:10.1029/2004JA010411.

Lincoln, J. V. (1977), Geomagnetic and solar data (errata), *J. Geophys. Res.*, *82*, 2893.

Lockwood, M., R. Stamper, and M. N. Wild (1999), A doubling of the Sun's coronal magnetic field during the last 100 years, *Nature*, *399*, 437.

Lockwood, M., A. P. Rouillard, I. Finch, and R. Stamper (2006), Comment on "The IDV index: Its derivation and use in inferring long-term variations of the interplanetary magnetic field strength" by Leif Svalgaard and Edward Cliver, *J. Geophys. Res.*, *111*, A09109, doi:10.1029/2006JA011640.

Lundstedt, H. (1984), Influence of interplanetary interaction regions on geomagnetic disturbances and tropospheric circulation, *Planet. Space Sci.*, *32*(12), 1541, doi:10.1016/0032-0633(84)90022-9.

Martini, D., and K. Mursula (2006), Correcting the geomagnetic *IHV* index of the Eskdalemuir observatory, *Ann. Geophys.*, *24*, 3411.

Mayaud, P. N. (1967), Calcul preliminaire d'indices *Km*, *Kn* et *Ks* ou *Am*, *An*, et *As*, mesures de l'activité magnétique a l'échelle mondiale et dans les hémispheres Nord et Sud, *Ann. Geophys.*, *23*, 585.

Mayaud, P. N. (1972), The *aa* index: a 100-year series characterizing the geomagnetic activity, *J. Geophys. Res.*, *77*, 6870.

Mayaud, P. N. (1973), A hundred year series of geomagnetic data, 1868–1967, indices *aa*, Storm sudden commencements, *IAGA Bull. 33*, 252 pp., IUGG Publ. Office, Paris.

Mayaud, P. N. (1980), *Derivation, Meaning, and Use of Geomagnetic Indices*, *Geophys. Monogr. Ser.*, vol. 22, AGU, Washington, D. C.

Moos, N. A. F. (1910), *Colaba Magnetic Data, 1846 to 1905, 2, The Phenomenon and its Discussion*, 782 pp., Cent. Govt. Press, Bombay.

Murayama, T., and K. Hakamada (1975), Effects of solar wind parameters on the development of magnetospheric substorms, *Planet. Space Sci.*, *23*, 75.

Mursula, K., and D. Martini (2006), Centennial increase in geomagnetic activity: Latitudinal differences and global estimates, *J. Geophys. Res.*, *111*, A08209, doi:10.1029/2005JA011549.

Mursula, K., D. Martini, and A. Karinen (2004), Did open solar magnetic field increase during the last 100 years: A reanalysis of geomagnetic activity, *Sol. Phys.*, *224*, 85.

Nevanlinna, H. (2004), Results of the Helsinki Magnetic Observatory, 1844–1912, *Ann. Geophys.*, *22*, 1691, Sref-ID:1432-0576/ag/2004-22-1691.

O'Brien, T. P., and R. L. McPherron (2002), Seasonal and diurnal variation of *Dst* dynamics, *J. Geophys. Res.*, *107*(A11), 1341, doi:10.1029/2002JA009435.

Parish, R. C. (1989), Comparison of linear regression methods when both variables contain error: Relation to clinical studies, *Ann. Pharmacother.*, *23*(11), 891.

Rosenberg, R. L., and P. J. Coleman Jr. (1969), Heliographic latitude dependence of the dominant polarity of the interplanetary magnetic field, *J. Geophys. Res.*, *74*, 5611.

Russell, C. T., and R. L. McPherron (1973), Semiannual variation of geomagnetic activity, *J. Geophys. Res.*, *78*, 92.

Russell, C. T., and T. Mulligan (1995), The 22-year variation of geomagnetic activity: Implications for the polar magnetic field of the Sun, *Geophys. Res. Lett.*, *22*(23), 3287, doi:10.1029/95GL03086.

Sargent, H. H., III (1986), The 27-day recurrence index, in *Solar Wind-Magnetosphere Coupling*, edited by Y. Kamide and J. A. Slavin, p. 143, Terra Sci., Tokyo.

Schmidt, A. (1905), Ergebnisse der magnetischen Beobactungen in Potsdam, *Veröffentl. des Preuss. Meteor. Inst.*, Berlin.

Snyder, C. W., M. Neugebauer, and U. R. Rao (1963), The solar wind velocity and its correlation with cosmic-ray variations and with solar and geomagnetic activity, *J. Geophys. Res.*, *68*, 6361.

Steen, A. S., N. Russeltvedt, and K. F. Wasserfall (1933), *The Scientific Results of the Norwegian Arctic Expedition in the Gjøa, 1903–1906*, part II, *Terrestrial Magnetism, Geofys. Publ.*, vol. 7, Grøndahl, Oslo, Norway.

Stozhkov, Y. I., and P. E. Pokrevsky (2001), Comments on a paper of H. S. Ahluvalia "On galactic cosmic ray flux decrease near solar activity minimum and IMF intensity," *Geophys. Res. Lett.*, *28*, 947.

Svalgaard, L. (1977), Geomagnetic activity: Dependence on solar wind parameters, in *Skylab Workshop Monograph on Coronal Holes*, edited by J. B. Zirker, chap. 9, p. 371, Columbia Univ. Press, New York.

Svalgaard, L., and E. W. Cliver (2005), The *IDV* index: Its derivation and use in inferring long-term variations of the interplanetary magnetic field strength, *J. Geophys. Res.*, *110*, A12103, doi:10.1029/2005JA011203.

Svalgaard, L., and E. W. Cliver (2006), Reply to the comment by M. Lockwood et al. on "The *IDV* index: Its derivation and use in inferring long-term variations of the interplanetary magnetic field strength," *J. Geophys. Res.*, *111*, A09110, doi:10.1029/2006JA011678.

Svalgaard, L., and E. W. Cliver (2007), Calibrating the sunspot number using "the magnetic needle," *Eos Trans. AGU*, *88*(23), Jt. Assem. Suppl., Abstract SH54B-02.

Svalgaard, L., E. W. Cliver, and A. Ling (2002), The semiannual variation of great geomagnetic storms, *Geophys. Res. Lett.*, *29*(16), 1765, doi:10.1029/2001GL014145.

Svalgaard, L., E. W. Cliver, and Le P. Sager (2003), Determination of interplanetary magnetic field strength, solar wind speed, and EUV irradiance, 1890–2003, in *Proceedings of ISCS 2003 Symposium: Solar Variability as an Input to the Earth's Environment*, *Eur. Space Agency Spec. Publ.*, ESA SP-535 15.

Svalgaard, L., E. W. Cliver, and P. Le Sager (2004), *IHV*: A new long-term geomagnetic index, *Adv. Space. Res.*, *34*, 436.

van Sabben, D., (Ed.) (1977), Geomagnetic data 1977: Indices, rapid variations, special intervals, *IAGA Bull. 32h.*, IUGG Publ., Paris.

Wilcox, J. M., and P. H. Scherrer (1972), Annual and solar magnetic cycle variations in the interplanetary magnetic field 1926–1971, *J. Geophys. Res.*, *77*, 5385.

————————————

E. W. Cliver, Air Force Research Laboratory, Hanscom Air Force Base, Bedford, MA 01731, USA. (edward.cliver@hanscom.af.mil)

L. Svalgaard, Easy Toolkit, Inc., 6927 Lawler Ridge, Houston, TX 77055, USA. (leif@leif.org)